



HAL
open science

C and O isotope compositions of modern fresh-water mollusc shells and river waters from Himalaya and Ganga plain

Ananta Prasad Gajurel, Christian France-Lanord, Pascale Huyghe, Caroline Guilmette, Damayanti Gurung

► **To cite this version:**

Ananta Prasad Gajurel, Christian France-Lanord, Pascale Huyghe, Caroline Guilmette, Damayanti Gurung. C and O isotope compositions of modern fresh-water mollusc shells and river waters from Himalaya and Ganga plain. *Chemical Geology*, 2006, 233 (1-2), pp.156-183. hal-00103698

HAL Id: hal-00103698

<https://hal.science/hal-00103698>

Submitted on 5 Oct 2006

HAL is a multi-disciplinary open access archive for the deposit and dissemination of scientific research documents, whether they are published or not. The documents may come from teaching and research institutions in France or abroad, or from public or private research centers.

L'archive ouverte pluridisciplinaire **HAL**, est destinée au dépôt et à la diffusion de documents scientifiques de niveau recherche, publiés ou non, émanant des établissements d'enseignement et de recherche français ou étrangers, des laboratoires publics ou privés.

**C and O isotope compositions of modern fresh-water mollusc shells and river waters
from Himalaya and Ganga plain**

**Ananta Prasad Gajurel^{a,b}, Christian France-Lanord^c, Pascale Huyghe^{b,*}, Caroline Guilmette^c,
Damayanti Gurung^d**

^a Department of Geology, Tri-Chandra Campus, Tribhuvan University, Kathmandu, Nepal

^b Université Joseph Fourier, LGCA/CNRS, Grenoble, France,

^c CRPG/CNRS, Vandoeuvre les Nancy, France,

^d Department of Geology, Kirtipur Campus, Tribhuvan University, Kathmandu, Nepal

* Corresponding author. Fax: +33 4 76 51 40 58

E-mail adresse huyghe@ujf-grenoble.fr

Abstract

The aim of this paper is to unfold the relationship between O and C isotope compositions of modern fresh-water mollusc shells and water in order to refine the basis of interpretation for paleoenvironmental reconstruction in the sub-Himalayan river basins. Large number of mollusc shells and associated host water from both running water and closed body of water were analysed including intra-shell variability in a few cases.

The O isotopic compositions of river waters in the Himalayas and Ganga plain have a large range, from -18‰ in the north of the High range up to -8 to -4 ‰ in the Ganga plain. $\delta^{18}\text{O}$ of rivers are also seasonally variable, especially in foothills rivers whereas the seasonal contrast is smoothed out for main Himalayan rivers having large catchments. O isotopic compositions of bulk shells (Aragonite) vary between -15 and -5 ‰. Average $\delta^{18}\text{O}_{\text{Ara}}$ values are consistent with precipitation at equilibrium with host waters at a temperature range of 20-25 °C suggesting that shell growth may be favoured during non-monsoon conditions. Shells collected along main Himalayan rivers have $\delta^{18}\text{O}$ values uniformly distributed within -11 and -6 ‰ reflecting the minimal seasonal contrast shown by these rivers. In contrast, O isotopic compositions of shells from foothills rivers vary only by 4 ‰. This shows that, depending on the type of river where the molluscs grow, the information in term of $\delta^{18}\text{O}$ amplitude will be different for identical climatic conditions. In closed or pond water bodies significant enrichment in ^{18}O due to evaporation is observed.

The C isotopic compositions of river dissolved inorganic carbon (DIC) decrease downstream from 0 to -10 ‰ reflecting input of soil derived alkalinity and plant productivity in the river. $\delta^{13}\text{C}$ of shells are systematically lower than compositions calculated for equilibrium with river DIC indicating that in addition to DIC, a significant fraction of carbon is derived from metabolic sources. Intra-shell $\delta^{13}\text{C}$ are stable compared to the seasonal variability of DIC suggesting that the pool of organic carbon changes throughout year.

Keywords

C and O isotopes, fresh-water molluscs, modern rivers, Himalaya, Ganga, seasonality, running water versus pond water.

1. Introduction

29 Carbon and oxygen isotope compositions of carbonate skeletons have been extensively used for reconstructing
30 past environmental parameters (e.g. Lowenstam and Epstein, 1954; Woodruff et al., 1981; Shackleton, 1986;
31 Miller et al., 1987). From a study of marine mollusc shells and their ambient marine waters, Lécuyer et al. (2004)
32 demonstrated that the oxygen isotope compositions of shells from most fossil mollusc species are suitable to
33 estimate past seawater temperatures. In river systems, mollusc shells represent remarkable sources of
34 geochemical information and allow to document seasonal variations through detailed analysis of growth layers
35 (e.g. Abell, 1985; Fritz and Poplawski, 1974; Dettman et al., 1999; Kaandorp et al., 2003). Nonetheless, only few
36 studies provide stable isotope data of laboratory-reared or natural shells along with their ambient waters
37 (Grossman and Ku, 1986; Margosian et al., 1987; Weidman et al., 1994; Klein et al., 1996).

38 Some studies have focussed on the reconstruction of paleo-environmental conditions in the Gangetic plain using
39 fossils from the plain and Siwaliks (Garzzone et al., 2000a; Dettman et al., 2001; Sharma et al., 2004; Gajurel et
40 al., 2003). These studies reveal a large variability in stable isotope compositions through time, and importantly
41 large seasonal cycle. Clearly, fossil records of fresh water mollusc represent a rich source of information to
42 document past evolution of river system. Our objective is to refine the basis of interpretation of oxygen and
43 carbon isotope compositions of fresh-water molluscs for paleoenvironmental reconstruction in the sub-
44 Himalayan river basin. For that purpose, we collected modern mollusc samples across a wide range in elevation,
45 from the Ganga Plain to the highest physiographic zones. Waters in the Himalayan rivers and in closed or
46 ponded bodies of water exhibit seasonal changes in temperature and stable isotope (C and O) compositions (Galy
47 and France-Lanord, 1999; Garzzone et al., 2000b). Therefore, we sampled several modern mollusc species from
48 streams/ivers and closed bodies of water of Himalayan Valleys and Ganga plain together with host water
49 samples and ambient temperature records to unfold the relationship between shell composition and water
50 parameters. In this paper, we compare water bodies in different geographical settings that differ primarily in the
51 size and elevation of their catchments: the Main Himalayan rivers draining complete Himalayan sections from
52 Tibet to the floodplain, small rivers originating from the Himalayan foothills, the main stream Ganga, and some
53 lakes, ponds and North Himalayan rivers.

54

55 **2. Setting: modern Himalayan drainage system and climate**

56

57 Three large rivers emerge from the Nepalese Himalayan belt and flow to the Ganga plain within ~300
58 km wide basin (Fig. 1): the Kosi, Narayani/Gandak and Karnali/Ghaghara rivers, in eastern, central and western

59 Nepal respectively. They drain a large part of Himalaya extending from North Himalaya (altitude 2500-4000 m
60 above mean sea level) through High Himalaya (>4000 m), Lesser Himalaya (300 to 3000 m) and Siwaliks (150-
61 1400 m) to the Ganga plain (less than 150-200 m). The headwaters of these large rivers are fed by melt water
62 from snow and glaciers. All of them, except the Arun, make 90° turns, flowing either eastward or westward
63 before crossing the Mahabharat Range, north of the trace of the Main Boundary Thrust (MBT). They then, flow
64 axially, sub-parallel to the MBT for more than 100 km and turn southward through the areas of structural
65 weakness to emerge in to the Ganga plain (Hagen, 1969; Seeber and Gornitz, 1983; Gupta, 1997). The Kosi,
66 Narayani and Karnali rivers have high average annual water discharge (varying between 1500 to 2000 m³/s)
67 (Sinha and Friend, 1994; DHM, 1998) and drain more than 75 % of the area of the Himalaya of Nepal. Their
68 sediment bed load form large modern alluvial megafans in the Ganga plain (Wells and Dorr, 1987; Sinha and
69 Friend, 1994). A few small rivers originate in the Lesser Himalaya, Siwalik foothills and within the Ganga plain.
70 They merge with the major rivers in the plain. They have smaller discharge and form interfans between the
71 megafans of the large rivers in the plain (Sinha and Friend, 1994). All the rivers of Nepal are tributaries of the
72 Ganga River. The main tributaries of the Ganga River originate from Himalaya although some flow from the
73 Indian shield representing less than 20% of the total Ganga discharge (Rao, 1979).

74 Our river water samples represent a wide range of climate with a characteristic pattern of temperature.
75 In the central Ganga plain average minimum and maximum temperatures are 8 and 21 °C for November-
76 February and 27 to 33 °C for March-June (Sharma et al., 2004). Surface air temperature records for more than 16
77 years (DHM, 2002) near the northern margin of the Ganga plain and in the Dun Valleys show more or less
78 similar climate with monthly maximum average temperatures of 36 °C for the April to September period
79 (summer) and 26 °C for the October to March period (winter). Tansen, Pokhara and Kathmandu in Lesser
80 Himalaya have mean values of 28 °C, 30 °C and 29 °C during the summer period and 20 °C, 23 °C and 22 °C
81 during the winter period. In North Himalayan valley (Jomsom), the mean annual minimum and maximum
82 temperatures are 5.3 °C and 17.5 °C, respectively.

83 Nepal receives about 80 % of the total annual precipitation during the June-September monsoon (DHM,
84 2002). Average annual precipitation in North Himalayan valley (Jomsom) is 257 mm. High annual rainfall
85 (>3000 mm) occurs in the Arun and Indrawati river headwaters (High Himalaya). The average wet and dry
86 season precipitations in Pokhara are 3934 and 157 mm, respectively. The highest annual precipitation is recorded
87 in the Pokhara valley, which lies within the catchment of the Narayani River system while the Karnali River
88 system is located in a lower precipitation area (<2000 mm) (DHM, 2002). The Ganga plain and Dun Valleys

89 (Siwalik foothills) receive average precipitation of 1760-69 mm and 1875-99 mm during wet-dry periods,
90 respectively. The Ganga plain (in India) receives annual rainfall of 800-2000 mm (Sinha and Friend, 1994).

91

92 **3. Sampling strategy and fauna**

93

94 The sampling area covers (24° 30' N-28° 50' N) latitude and (83° E-88° 30' E) longitude while the
95 altitude ranges from 17 to 3576 m (Fig. 1). We collected freshwater modern molluscs from a wide range of
96 habitats including river shores, lake shores, ox-bow lakes and isolated ponds situated within North Himalaya,
97 Lesser Himalaya and Dun valleys, and the Ganga alluvial plain and Bangladesh delta plain. The sampled
98 specimens from the Ganga plain and Himalayan valleys can be easily identified (Subba Rao, 1989; Subba and
99 Ghosh, 2000; Neumann et al., 2001) and represent two genera from *Bivalvia* class and ten genera from
100 *Gastropoda* class whose widespread genus are *Bellamyia* sp. and *Melanoid* sp. (Fig. 2). They include living and
101 dead specimens. Mollusc's habitat water samples (host water) were collected while habitat water temperature
102 (ambient temperature), pH and air temperature were also recorded during sampling for most locations. The
103 favoured habitat of molluscs in this study are low current environment and closed or ponded environments. In
104 the case of ponds, fresh water as well as stagnant water samples were collected to examine the possible effect of
105 atmospheric exchange and evaporation on the carbon and oxygen isotopic compositions of the biogenic
106 carbonate. At several locations, members of different species were taken in order to examine the variability in
107 shell chemistry of different taxa living in the same environment, caused by different physiological effects and
108 growth periods.

109

110 **4. Analytical techniques**

111

112 *4.1 Water*

113

114 Meteoric water samples were collected daily at Kathmandu using a PVC collector. Special care was
115 taken to avoid evaporation. The fact that all samples lie close to the global meteoric water line confirms the
116 reliability of the sampling. When daily precipitation was lower than 1 mm we did not collect any sample. River
117 water samples were filtered on site through <0.2µm nylon membranes and stored in polyethylene bottles free of
118 air. The carbon isotopic compositions of dissolved inorganic carbon ($\delta^{13}\text{C}_{\text{DIC}}$) were measured on CO_2 released by

119 acidification with H_3PO_4 in vacuum. Aliquots of 15 to 20 ml were injected into the reaction vessel through a
120 septum. The CO_2 released after acidification was extracted while water was trapped as ice (-80 to -50°C). The
121 outgassing procedure was repeated three times in order to extract most of the DIC from the water. Total CO_2
122 released was measured manometrically for DIC concentration and analysed for $^{13}\text{C}/^{12}\text{C}$ ratio using a modified VG
123 602D isotope ratio mass spectrometer. Results are expressed as $\delta^{13}\text{C}_{\text{DIC}}$ relative to PDB and the overall
124 reproducibility is $\pm 0.3\%$.

125 The oxygen isotopic composition of host water samples ($\delta^{18}\text{O}_\text{W}$) were analysed using the classical CO_2
126 equilibration method of Epstein and Mayeda (1953). One cm^3 of water was equilibrated in a vacuum container
127 sealed with a septum with CO_2 at 900 mbar and $25 \text{ }^\circ\text{C} \pm 0.1 \text{ }^\circ\text{C}$. $^{18}\text{O}/^{16}\text{O}$ ratios are expressed as $\delta^{18}\text{O}_\text{W}$ relative to
128 V-SMOW and overall analytical reproducibility is $\pm 0.1 \%$.

129 Hydrogen isotopic compositions of water samples were measured using a GV-Isoprime mass
130 spectrometer coupled to an elemental analyzer. 3 μl of water were injected over Cr reactor at 1100°C under He
131 flux and analysed in continuous flow mode. D/H ratios are expressed as δD relative to V-SMOW and overall
132 analytical reproducibility is better than $\pm 2 \%$.

133

134 *4.2 Mollusc shells*

135

136 Mollusc shell samples were cleaned in distilled water with ultrasound to remove adhered sediments and
137 organic debris. Before micro sampling, shell outer periostracum, which is composed of organic coloured layers,
138 were removed by scraping with the help of manual drilling bit to expose white prismatic layer. Intra-shell
139 samples were taken all along the profile parallel to the growth lines of intact shell. Typical width of growth
140 layers is 0.5 to 2 mm. Whole shell samples are either whole shell grinded for small specimens (one mm) or, for
141 larger ones, a slice perpendicular to the growth line covering the entire life span of the specimen.

142 For experimental analyses, three individual representative average samples of a *Bellamya bengalensis*
143 were treated in three different ways: one powder sample was vacuum roasted for one hour at $380 \text{ }^\circ\text{C}$ and another
144 sample was heated in plasma O_2 cold asher for one night to volatilize shell organic compounds and the third one
145 was not treated. These procedures did not produce any remarkable variation (Table 1). The samples were reacted
146 under vacuum with $\sim 100 \%$ phosphoric acid at $25 \pm 0.1 \text{ }^\circ\text{C}$ (McCrea, 1950). Isotopic analyses of the released
147 CO_2 were performed in a modified mass spectrometer model VG 602. Carbon and oxygen isotopic ratios of
148 aragonite are expressed as $\delta^{13}\text{C}_{\text{Ara}}$ and $\delta^{18}\text{O}_{\text{Ara}}$ relative to PDB. Following common practice for aragonite shell

149 analyses (e.g. Dettman et al, 1999; Lecuyer et al, 2004) we did not apply any correction specific for aragonite
150 and used the standard correction for calcite. Ten to fifteen repeated analyses of calcite international standards
151 over the analytical period are : NBS-18 $\delta^{13}\text{C} = -5.02 \pm 0.04 \text{ ‰}$ and $\delta^{18}\text{O} = -23.06 \pm 0.13 \text{ ‰}$, NBS-19 $\delta^{13}\text{C} =$
152 $2.00 \pm 0.04 \text{ ‰}$ and $\delta^{18}\text{O} = -2.15 \pm 0.13 \text{ ‰}$, IAEA -CO-1 $\delta^{13}\text{C} = 2.47 \pm 0.04 \text{ ‰}$ and $\delta^{18}\text{O} = -2.46 \pm 0.09 \text{ ‰}$, IAEA -CO-
153 $8 \delta^{13}\text{C} = -5.74 \pm 0.07 \text{ ‰}$ and $\delta^{18}\text{O} = -22.79 \pm 0.1 \text{ ‰}$. Overall reproducibility is $\pm 0.1 \text{ ‰}$.

154 Shell mineralogy was examined using X-Ray diffraction in which only aragonite was observed for
155 whole shell powders (n=3). The carbonate content of shells was calculated from manometrically measured CO_2
156 yields after complete reaction with phosphoric acid. Carbonate contents ranged from 95% to 99%.

157

158 **5. Results**

159

160 *5.1 Isotopic composition of waters*

161

162 Hydrogen and oxygen isotopic composition of waters (δD_w , $\delta^{18}\text{O}_w$) and carbon isotope ratio of DIC
163 ($\delta^{13}\text{C}_{\text{DIC}}$) are listed in table 2. Sample locations are listed in appendix 1 and 2. Additional isotopic data from
164 Ramesh and Sarin (1992), Jenkins et al. (1987) and Galy and France-Lanord (1999) have also been included.

165 The $\delta^{18}\text{O}_w$ values of rivers, lakes and ponds in the Himalayas and Ganga plain show a large range as seen in
166 figures 3 and 4 for different zones (North Himalaya, High Himalaya, Kathmandu Valley, Phewa Lake (Pokhara),
167 foothills, Main Himalayan rivers and Main Ganga River in the plain). Himalayan rivers display a strong
168 dependence on elevation with $\delta^{18}\text{O}_w$ around -18 ‰ to the north of the High range up to -8 to -4 ‰ in the Ganga
169 plain. Such a variability has already been reported by Ramesh and Sarin (1992) and Garziona et al. (2000b). The
170 large-scale variations observed from High Himalaya to the Ganga plain are controlled by the combined effects of
171 elevation, orographic precipitation and temperature. Orographic precipitation drives a strong Rayleigh
172 distillation, which tends to deplete the clouds remaining over the north Himalaya in the heavy isotope. In
173 parallel, temperatures strongly decrease from the plain to the high range amplifying this trend.

174 $\delta^{18}\text{O}_w$ of rivers are also seasonally variable. Monsoon rain can be 4 ‰ lower than precipitation during
175 the dry season as obviously observed in foothills rivers (Fig. 4). Over the whole basin, $\delta^{18}\text{O}$ of monsoon rains are
176 markedly lower compared to precipitations during the rest of the year. This is well documented in the Gangetic
177 plain and is related to the "amount effect" or intensity of precipitation (Rozanski et al., 1993; Bhattacharya et al.,
178 2003). Our record of precipitation at Kathmandu over the year 2001-02 (appendix 3, Fig. 5) shows a similar

179 seasonal evolution. For Kathmandu, the $\delta^{18}\text{O}$ values of precipitation are close to 0‰ and even positive
180 throughout the dry season, after which they drop abruptly to the range of -5 to -15‰ at the onset of the monsoon
181 season. The variation is clearly correlated with the intensity of precipitation. The weighted average $\delta^{18}\text{O}$ values is
182 -7.9 ‰ for the whole year and that of the monsoon period is -10.6 ‰. This sharp seasonal contrast is smoothed
183 in the river signal, especially for large area catchments as observed for the Ghaghara, Narayani-Gandak and Kosi
184 rivers. For the Narayani-Gandak, which is most extensively monitored, the difference between dry and wet
185 seasons does not exceed 3 ‰. In the floodplain, the Ganga shows a clear seasonal contrast in the western part up
186 to Patna (Fig. 3b). Dry season compositions are between -6 to -4 ‰ whereas during monsoon they vary between
187 -8 to -10 ‰. This difference results from both the lower $\delta^{18}\text{O}$ values of monsoon precipitation and the greater
188 influx of Himalayan water during the monsoon as the $\delta^{18}\text{O}$ of precipitation is lower in the Himalaya than on the
189 plain. At the outflow in Bangladesh, the Ganga is usually \sim -10 ‰ during monsoon. Values as high as -7 ‰ have
190 been reached during the 2004 monsoon, probably due to large rainfall amounts on the Ganga Plain during that
191 period. The Gomti (Table 2), which is a plain fed river, appears stable and is around -7 ‰ throughout the year.
192 This stability is probably related to a discharge of local groundwater (Bhattacharya et al., 1985; Sinha and
193 Friend, 1994).

194 During the dry season, evaporation in the floodplain can significantly affect the O and H isotopic
195 compositions (Krishnamurthy and Bhattacharya, 1991; Ramesh and Sarin, 1992). This is shown by compositions
196 lying below the meteoric water line in a $\delta^{18}\text{O}$ vs. δD diagram (Fig. 6). We observe a similar trend for Ganga
197 water in May 2004 (Table 2) whereas Main Himalayan rivers such as the Ghaghara, Gandak and Kosi show no
198 significant effect of evaporation. Monsoon compositions in the floodplain show no shift from the meteoric
199 waterline. Similarly, North Himalayan rivers and Kathmandu Valley rivers show no evidence for evaporation
200 (Fig. 6) except for minor catchments in the Kathmandu Valley during monsoon (Jenkins et al., 1987). Finally, we
201 observe major effects of evaporation for ponds located in the floodplain and Himalaya (Fig. 6). It is important to
202 document these effects as ponds are quiet environment favourable to the development of gastropods.

203 $\delta^{13}\text{C}_{\text{DIC}}$ values of river water are also highly variable (Table 2, Fig. 7). They have very high values in the
204 North Himalaya around 0 ‰ and decrease downstream toward values around -5 to -8 ‰ for the Main Himalayan
205 rivers. In Northern Himalaya where biological activity is limited, sulfuric acid released by sulfur oxidation is a
206 significant source of acid for carbonate dissolution (Galy and France-Lanord, 1999). It produces DIC close to 0
207 ‰ without noticeable contribution of soil organic CO_2 since most carbonates are of marine origin. Downstream
208 $\delta^{13}\text{C}_{\text{DIC}}$ values become significantly lower (between -5 to -10 ‰) reflecting input of soil derived alkalinity in the

209 river (Galy and France-Lanord, 1999). However, in High Himalaya, hot springs enriched in alkalinity derived
210 from outgassing of metamorphic CO₂ towards surface contribute to maintain relatively high $\delta^{13}\text{C}_{\text{DIC}}$. Due to
211 carbonate precipitation and CO₂ outgassing, these springs have very high $\delta^{13}\text{C}_{\text{DIC}}$ up to +15 ‰ and, when mixed
212 with river water, tend to increase their $\delta^{13}\text{C}_{\text{DIC}}$. Altogether, about 10 % of the riverine DIC in Himalaya could be
213 derived from thermal spring activity (Evans et al., 2004). Siwaliks drainage basins have lower $\delta^{13}\text{C}$ values
214 around -8 to -10 ‰. The main Himalayan tributaries of the Ganga (Gandak and Kosi) have $\delta^{13}\text{C}_{\text{DIC}}$ values around
215 -7 to -9 ‰. In the Ganga plain, the Ganga varies from relatively high values in the West (-3 to -6 ‰) to more
216 depleted values around -6 to -10 ‰ downstream under the combined influence of (1) Himalayan river input, (2)
217 increase of silicate weathering in the soils of the floodplain and (3) increased plant productivity in the eastern
218 part of the Gangetic plain.

219 Except for a few cases, there is a systematic difference between monsoon and dry season waters, the latter
220 showing higher $\delta^{13}\text{C}_{\text{DIC}}$ (Table 2). This difference varies between 0 and 5 ‰ and derives from complex controls
221 between origin of water (Himalayan vs. plain) and time of residence of water in soils. It is noticed that the
222 variability is relatively large in Bangladesh (Fig 8). The Ganga $\delta^{13}\text{C}_{\text{DIC}}$ values during the monsoon vary from -10
223 to -7.3 ‰. $\delta^{13}\text{C}_{\text{DIC}}$ in the Ganga are well correlated with $\delta^{18}\text{O}$ of water with low $\delta^{13}\text{C}_{\text{DIC}}$ being associated with
224 low $\delta^{18}\text{O}_\text{w}$. The latter reflects higher contribution of Himalayan waters.

225

226 *5.2 Isotopic composition of aragonite shells*

227

228 All isotopic data are given in table 3 and summarized in figures 4 and 7 in the form of histograms for
229 different geographical environments. Water isotopic compositions are compared to shell aragonite composition.
230 For oxygen, isotopic compositions of water relative to V-SMOW are compared to aragonite composition relative
231 to PDB.

232

233 *5.2.1. Bulk oxygen isotopic composition of shells*

234

235 $\delta^{18}\text{O}$ values of bulk shells vary between -15 and -5 ‰ for running water environment. The lowest value
236 of -15.2 ‰ is associated with low $\delta^{18}\text{O}$ waters from North Himalaya. Samples from ponds display higher values
237 between -8 and +3 ‰ that are related to ^{18}O enrichment by evaporation in closed system environment.

238 In discussing this data set we define three groups based on the characteristic of the river water isotopic
239 composition. Foothills samples belong to local watershed in the Lesser Himalaya and Siwaliks where waters are
240 characterized by marked seasonality. The Main Himalayan rivers are made up of the samples from the Karnali-
241 Ghaghara, Narayani-Gandak and Kosi from the foothills to their confluence with the Ganga. Their $\delta^{18}\text{O}_W$ values
242 are relatively similar and stable throughout the seasons. The third group consists of main Ganga samples for which
243 waters have higher and more variable $\delta^{18}\text{O}_W$ than Main Himalayan rivers (Fig. 3b). Data of $\delta^{18}\text{O}_{\text{Ara}}$ for these three
244 groups are represented in the form of histograms in figure 4.

245 Foothills gastropods show a clear unimodal distribution between -10 and -6 ‰ and centered on -8 ‰.
246 Main Himalayan river gastropods have $\delta^{18}\text{O}_{\text{Ara}}$ values uniformly distributed between -12 and -5 ‰. In contrast to
247 foothills samples, this range is greater than and encompasses their host waters ($\delta^{18}\text{O}_W = -10$ to -6 ‰). Fourteen
248 samples representing three species *Bellamyia bengalensis*, *Digoniostoma textum* and *Indoplanorbis* sp. have been
249 taken at the same location on the Ghaghara bank. All of them show higher variability than the whole dataset of
250 the Main Himalayan rivers. No significant difference occurs among the species *Bellamyia bengalensis*,
251 *Digoniostoma textum* and *Indoplanorbis* sp. For the Main Ganga stream, most samples cluster between -8 and -5
252 ‰ and only few samples have lower values around -9 ‰. Ten *Bellamyia bengalensis* specimens sampled on the
253 Ganga at Barauni (BR-316) are quite homogeneous between -8.1 and -6 ‰. Altogether, the average $\delta^{18}\text{O}_{\text{Ara}}$ for the
254 Ganga is -6.4 ‰ ($\sigma=1.0$), which is significantly higher than that of Main Himalayan rivers at -8.8 ‰ ($\sigma=2.3$) or
255 foothills rivers at -7.6 ‰ ($\sigma=1.1$). The Gomti river which is draining only the plain, shows values very similar to
256 those of the main Ganga stream with an average value of -7.0 ‰ ($\sigma=1.0$). In the plain, samples from ponds display
257 highly variable $\delta^{18}\text{O}_{\text{Ara}}$ values from -8 ‰ up to +3 ‰. Low values are in the range of river values whereas high
258 values show clear effect of ^{18}O enrichment due to evaporation of closed water bodies. In the range, samples from
259 the Phewa Lake (Pokhara) which is not significantly evaporated have homogeneous compositions with an average
260 $\delta^{18}\text{O}_{\text{Ara}}$ at -8.6 ‰ ($\sigma=0.8$). The few samples collected in North Himalayan rivers show the lowest $\delta^{18}\text{O}_{\text{Ara}}$ between
261 -15 and -8 ‰ consistent with the lower composition of the host waters.

262 5.2.2. Carbon isotopic composition of shells

263
264
265 Except one sample from North Himalaya, all $\delta^{13}\text{C}_{\text{Ara}}$ of shell samples collected from rivers are between -13 and -4
266 ‰. The average $\delta^{13}\text{C}_{\text{Ara}}$ is -7.6 ‰ with a standard deviation of 2.0, which shows that the overall variability is low.
267 The highest values are observed in the western Ganga and the rivers with dominant plain input (Gomti and Rapti).
268 On the contrary, the lowest values are observed in the foothills rivers. This group is the only one that significantly

269 differs from the others with an average composition of -9.7 ‰ ($\sigma=2.1$). All other groups have average $\delta^{13}\text{C}_{\text{Ara}}$
270 between -7.7 and -6.6 ‰ . For all groups analysed, we observe no relationship between $\delta^{18}\text{O}_{\text{Ara}}$ and $\delta^{13}\text{C}_{\text{Ara}}$.

271
272 *5.2.3 Intra-shell compositions*

273
274 We analysed four samples to document intra-shell isotopic variations due to seasonal effect during
275 growth. Such variations have been reported for fossil samples of the Ganga plain (Sharma et al, 2004) and of the
276 Siwaliks (Dettman et al. 2001). Data are listed in table 4 and presented in figures 9, 10a and 10b. Both molluscs
277 from the plain (BR-316-10 from the Ganga and BR 337-3 from the Gandak) and bivalve (Btw-2 cor) from the
278 Tinau khola foothills river show marked variations with increasing $\delta^{18}\text{O}_{\text{Ara}}$ during shell growth. For these samples
279 the amplitude of the increase is about 3 ‰ . The fact that $\delta^{18}\text{O}_{\text{Ara}}$ simply increases and does not return to more
280 negative values suggests that these specimens lived for only one season. Another sample from a foothills river
281 (Chit 1) shows only limited variation of about 1 ‰ . $\delta^{13}\text{C}_{\text{Ara}}$ values are rather stable and independent of $\delta^{18}\text{O}_{\text{Ara}}$
282 with values around -8 ‰ for both BR-316-10 and Chit-1, and -11 ‰ for Btw-2 cor.

283
284 **6. Discussion**

285
286 *6.1 Oxygen isotope fractionation between biogenic carbonate and water*

287
288 Stable oxygen isotopic composition of biogenic carbonate is controlled by both temperature and isotopic
289 composition of environmental water during shell accretion (e.g. Epstein et al., 1953). The measured $\delta^{18}\text{O}$ values
290 of mollusc shells and water and ambient temperature of water are examined to oxygen isotope equilibrium
291 fractionation between carbonate and water. We used the fractionation-temperature relationship of Dettman et al.
292 (1999) that is based on calibration from Grossman and Ku (1986):

293
$$1000 \ln \alpha = (2.559 \cdot 10^6 / T^2) + 0.715$$

294 where T is the temperature of water in $^{\circ}\text{K}$ and α is the fractionation coefficient between water (w) and aragonite
295 (Ara).

296 The analysis of $\delta^{18}\text{O}_{\text{W}} - \delta^{18}\text{O}_{\text{Ara}}$ relationship ideally requires a detailed record of $\delta^{18}\text{O}_{\text{W}}$ and temperature
297 variations, which is not available for most settings studied here. We calculated $\delta^{18}\text{O}_{\text{Ara}}$ from $\delta^{18}\text{O}_{\text{W}}$ for the
298 different main settings that we sampled (Bangladesh Ganga, Central Ganga plain, Main Himalayan rivers,

299 foothills rivers). For this purpose, we used all $\delta^{18}\text{O}_w$ data available (Table 2 and Ramesh and Sarin, 1992). For
300 the data of Ramesh and Sarin (1992), no temperatures were available and we used estimates based on standard
301 seasonal temperatures. Figure 11 shows that the Ganga is expected to generate aragonite with marked seasonal
302 change in $\delta^{18}\text{O}$ at least in the Central Ganga plain area where there is a potential variation of $\sim 4\text{‰}$ between the
303 winter and the monsoon seasons. The main Himalayan rivers show lower amplitude than the Ganga as expected
304 from the relative insensitivity of their $\delta^{18}\text{O}_w$. From this limited data set, no significant difference is expected
305 among these rivers. The Gandak and Kosi appear very similar and the Ghaghara is systematically higher than its
306 two eastern analogs. Foothills rivers are expected to show the highest seasonal contrast in $\delta^{18}\text{O}$ with 6 to 7 ‰
307 between April and the monsoon.

308

309 6.1.1 Intra-shell data

310

311 *Bellamya bengalensis* sample BR 316-10 from the Eastern Ganga shows a clear evolution from the apex
312 around -10‰ to -7‰ towards the aperture (Fig. 9). Comparing these values with the model $\delta^{18}\text{O}_{\text{Ara}}$ for Ganga
313 (Fig 11), it appears that the lowest $\delta^{18}\text{O}_{\text{Ara}}$ of the apex is close to the expected value in the monsoon period. It
314 would imply that the increase in $\delta^{18}\text{O}_{\text{Ara}}$ up to -7‰ corresponds to the subsequent autumn season. The measured
315 amplitude is however lower than the calculated one and winter composition as high as -4‰ is not observed in
316 this sample. It is to be noted that because of the shell shape, the apex that records the monsoon low $\delta^{18}\text{O}_{\text{Ara}}$ value
317 represents only a minor proportion of the total shell. As a consequence, the bulk composition is controlled by the
318 autumn aragonite and is around -7.5‰ .

319 The articulated bivalve *Corbicula* sp (Btw-2 cor) sampled from shore sediments of the foothills river
320 (Tinau Khola) shows lower $\delta^{18}\text{O}_{\text{Ara}}$ value (Fig. 10b), which is slightly higher than the minimum $\delta^{18}\text{O}_{\text{Ara}}$ values
321 calculated for the monsoon in foothills rivers. The overall variability in $\delta^{18}\text{O}_{\text{Ara}}$ shown by the mollusc is 2.8‰ ,
322 which is lower than the $5\text{-}6\text{‰}$ range calculated for foothills rivers. This may reflect a lifespan shorter than the
323 whole year as suggested by the lack of reverse trend of the growth record. Integrating effect of growth may also
324 tend to blur the effective ambient water variability. For the gastropod *Brotia* sp. (Fig. 10a) sampled from the
325 foothills Rapti river (Chit 1), the recorded $\delta^{18}\text{O}_{\text{Ara}}$ values around -8‰ are incompatible with the monsoon period
326 in foothills rivers and slightly lower than the range calculated for the winter period. They could reflect growth
327 during the warm period prior to the monsoon.

328

329 6.1.2 Bulk shells data

330

331 Bulk shell data do not allow a detailed analysis of water to carbonate relationship because rivers are
332 seasonally variable and bulk analyses integrate a specific intra-shell variability. Therefore we will analyse each
333 setting separately according to its own characteristics.

334 In environments where $\delta^{18}\text{O}_W$ is relatively stable such as the Phewa Lake (Pokhara) and the Gomti
335 River in the floodplain, $\delta^{18}\text{O}_{\text{Ara}}$ of shells show limited variability around $-8.6\text{‰} \pm 1$ and $-7.0\text{‰} \pm 1$ respectively.
336 Based on aragonite-water fractionation of Dettman et al. (1999) and on the average $\delta^{18}\text{O}_W$ value, we calculate an
337 apparent temperature of precipitation between 20 and 30 °C which corresponds to major part of the seasonal
338 range of temperatures in these two sites (Fig. 12).

339 In other environments, $\delta^{18}\text{O}$ values of rivers are more variable and the comparison of water and shell
340 $\delta^{18}\text{O}$ values highlights some characteristics of the different groups (Fig 4). For a given zone, we compare the set
341 of shell data to the $\delta^{18}\text{O}_W$ values and average temperature of waters at different seasons. Winter temperatures are
342 around 15-20 °C in rivers of foothills and floodplain. For these temperatures, aragonite-water fractionation
343 coefficient is between 1.031 and 1.032 implying that $\delta^{18}\text{O}_{\text{Ara}}^{\text{PDB}}$ is equal to $\delta^{18}\text{O}_W^{\text{SMOW}}$ or 1 ‰ lower. Pre-
344 monsoon and monsoon temperatures are very high around 25-32 °C (aragonite-water fractionation coefficient
345 between 1.028 and 1.030), which leads to $\delta^{18}\text{O}_{\text{Ara}}^{\text{PDB}}$ being 1 to 2 ‰ lower than $\delta^{18}\text{O}_{\text{water}}^{\text{SMOW}}$.

346 For samples from foothills rivers, $\delta^{18}\text{O}_{\text{Ara}}$ are relatively homogeneous around -7 ‰ which is compatible
347 with winter and pre-monsoon waters and conditions. Monsoon waters in these watersheds have significantly
348 depleted compositions which should lead to shells with compositions around -11 to -13 ‰ (Fig. 11). Monsoon
349 compositions are therefore not recorded or represent only a minor proportion of these shells. This could be
350 similar to what is observed for intra-shell variability in sample BR-316-10 where only a small fraction of the
351 shell records monsoon composition.

352 The group of Main Himalayan rivers shows $\delta^{18}\text{O}_W$ values between -10 and -6 ‰. Using a temperature
353 of 20 °C during winter, and 30 °C during the warm season and monsoon, $\delta^{18}\text{O}_{\text{Ara}}$ values of the shells should be
354 between -10 to -8 ‰ during winter and -13 to -10 ‰ during monsoon (Fig. 11). Nineteen samples out of twenty-
355 five are compatible with these ranges of values. More significantly, fifty percent of bulk gastropod data have
356 $\delta^{18}\text{O}$ values lower than -10 ‰, implying that for these samples, most of the aragonite shell was generated during
357 the monsoon period. Six samples have $\delta^{18}\text{O}$ higher than -8 ‰, which are incompatible with any measured range
358 of waters composition and temperatures. While we have no satisfying explanation for these samples, the most

359 plausible one is that they correspond to shells which grew in shallow pools near a riverside which were subject to
360 isotopic enrichment by evaporation. Such shells could then have been transported back in the main river during
361 the high flow of the monsoon.

362 Ganga samples have bulk $\delta^{18}\text{O}_{\text{Ara}}$ that cluster around -6 ‰ which suggests that most of the aragonite has
363 been formed with high $\delta^{18}\text{O}$ waters of the Ganga during winter or pre-monsoon period. Most monsoon Ganga
364 waters have low $\delta^{18}\text{O}$ due to ^{18}O depleted monsoon precipitation and Himalayan rivers input. Combined with
365 high temperature in the Gangetic plain these conditions should generate aragonite lower than -9 ‰ which is not
366 observed.

367

368 *6.1.3 Average compositions*

369

370 One can also compare average compositions of the different geographical groups for both water and
371 shell samples in a $\delta^{18}\text{O}_{\text{W}}$ vs. $\delta^{18}\text{O}_{\text{Ara}}$ diagram (Fig. 12). In such a diagram data should align on equilibrium lines
372 depending on temperature. While variability is rather large for most groups, we observe that different groups
373 tend to align along the 20°C equilibrium line which supports a general compatibility with non monsoon
374 conditions. In the same diagram, data for North Himalayan samples show that they reflect significantly lower
375 temperatures. This comparison underlines the differences existing between shells grown in Main Himalayan
376 rivers on one side and Ganga mainstream, foothills and plain rivers on the other side. Main Himalayan rivers are
377 continuously supplied by ^{18}O depleted High Himalayan watershed resulting in shells with 1-1.5 ‰ lower average
378 $\delta^{18}\text{O}$ values than shells from foothills and plain.

379

380 *6.2 Carbon isotope fractionation between biogenic carbonate and water*

381

382 Gastropods principally uptake carbonate from dissolved inorganic carbon of water to build their shell.
383 Carbon isotopic fractionation between aragonite and HCO_3^- is 2.6 ± 0.6 between 10 and 40°C (Rubinson and
384 Clayton, 1969; Romaneck et al., 1992). Therefore, the $\delta^{13}\text{C}$ of aragonite should be at least 2 ‰ higher than that
385 of DIC in ambient river water. An examination of our data set shows that this is not the case for most of our
386 samples (Fig. 7). Overall they have $\delta^{13}\text{C}_{\text{Ara}}$ equal to or 1 to 2 ‰ lower than that of DIC at sampling site. This is
387 also confirmed by noting that average $\delta^{13}\text{C}$ values of the different groups (Fig. 13) are 2 to 3 ‰ lower than that
388 expected from DIC values of corresponding river waters.

389 The discrepancy between measured and calculated $\delta^{13}\text{C}_{\text{Ara}}$ could be due to non-representative sampling
390 of DIC. But at least in cases of the Ganga and the Narayani-Gandak, seasonal cover was sufficient to rule out a
391 possible bias of sampling. A second source of bias is related to the speciation of carbon in water. All samples
392 have pH around 8 ± 0.55 implying that most of DIC is present as HCO_3^- . However, these rivers have total DIC,
393 which is 10 to 15 % in excess of the measured alkalinity (Galy and France-Lanord, 1999). This means that a
394 significant proportion of DIC is present as excess CO_2 with $\delta^{13}\text{C} \sim 8 \text{ ‰}$ lower than that of HCO_3^- . The effective
395 HCO_3^- is therefore expected to be about 0.5 to 1 ‰ higher than the measured DIC, leading to higher $\delta^{13}\text{C}$ values
396 in precipitating aragonite and therefore larger discrepancy with measured $\delta^{13}\text{C}_{\text{Ara}}$.

397 The difference between the calculated and observed $\delta^{13}\text{C}_{\text{Ara}}$ values is known from earlier studies and is
398 commonly explained by the incorporation of metabolic CO_2 from respiratory sources (e.g. Michener and Shell,
399 1994; Dettman et al., 1999; Aucour et al., 2003). Such C can be provided by digestion of particulate organic
400 carbon (POC) of land origin or phytoplankton of the river. POC in the Ganga rivers has low $\delta^{13}\text{C}$ value around -
401 22‰ (Aucour et al., in press) and therefore represents a source of low $\delta^{13}\text{C}$ CO_2 . Phytoplankton $\delta^{13}\text{C}$ is still not
402 documented but is likely to be around -30‰ assuming a DIC-phytoplankton fractionation around 22‰. The
403 proportion of inorganic to organic carbon incorporated in the shell is a matter of debate and several estimations
404 have been developed (McConnaughey et al., 1997; Aucour et al. 2003). Following Aucour et al. (2003) about 30
405 to 70% of total carbon should be of metabolic origin in order to explain our observed shell compositions
406 assuming that POC is the only organic source with $\delta^{13}\text{C}$ of -22‰. Uncertainties are large mostly because each
407 type of site displays a relatively large range of $\delta^{13}\text{C}_{\text{DIC}}$ and $\delta^{13}\text{C}_{\text{Ara}}$. These proportions are of course lower if
408 phytoplankton is ingested instead of POC.

409 The $\delta^{13}\text{C}_{\text{DIC}}$ of rivers tends to be lower during the monsoon period with a typical contrast of 2 to 3 ‰
410 between the monsoon and dry season for both Ganga and Main Himalayan Rivers (Fig. 7). This should generate
411 a seasonal trend in the $\delta^{13}\text{C}_{\text{Ara}}$ of shell that is not observed. The Ganga sample BR 316-10 (Fig. 9) for which
412 intra-shell variation of $\delta^{18}\text{O}$ is consistent with a monsoon to dry season evolution does not show a parallel trend
413 for carbon isotopes. $\delta^{13}\text{C}_{\text{Ara}}$ of this sample is rather stable around $-8 \text{ ‰} \pm 0.5$. Similarly the Gandak sample BR-
414 337-3 does not show any significant change in $\delta^{13}\text{C}_{\text{Ara}}$ that could reflect the seasonal evolution of $\delta^{13}\text{C}_{\text{DIC}}$ of this
415 river (-5 to -8 ‰). This suggests a complex interplay of changes in the source of organic carbon and its
416 incorporation in the shell over the year. One hypothesis is that the seasonal DIC contrast is counterbalanced by a
417 change of the organic carbon sources. During the monsoon, suspended particles concentrations are very high (1
418 to 5 g/l unpublished data) and POC around -22 ‰ dominates the organic pool. On the contrary, during the dry

419 season, suspended particle concentration decline to 0.1-0.2 g/l. This increases the proportion of phytoplankton
420 relative to POC in the organic carbon pool and could balance the increase in $\delta^{13}\text{C}_{\text{DIC}}$. Such hypothesis would
421 allow to maintain a relatively constant proportion of organic carbon during the year around 30 to 50 % of the
422 total carbon.

423

424 **7. Conclusion and implications for fossil record**

425 The main objective of this study was to determine how oxygen and carbon isotope compositions of
426 mollusc shell can document environmental conditions in the Gangetic plain. For the first time, isotopic
427 characteristics of river water in the Gangetic floodplain have been analysed for their seasonal variability and
428 their relation to the watershed size. This basis allows to determine how shells of freshwater molluscs can record
429 the isotopic compositions of river waters and how far we can relate it to climatic conditions.

430 Two distinct environments for the freshwater molluscs in the Ganga plain are observed. One is related
431 to flowing river and the other is stagnant water mass in isolated ponds. In rivers, average $\delta^{18}\text{O}_{\text{Ara}}$ values of shells
432 are found compatible with isotopic equilibrium with the waters at a temperature range of 20 to 25 °C. In contrast,
433 $\delta^{18}\text{O}$ values of shells from stagnant water bodies are highly variable and can reach values as high as +3 ‰ due to
434 the effect of evaporation. This effect has been observed in modern and quaternary lake and ponds of the Gangetic
435 plain (Sharma et al., 2004) as well as in the Mio-Pliocene Siwaliks (Dettman et al., 2001). Overall, river
436 molluscs have bulk $\delta^{18}\text{O}_{\text{Ara}}$ in the range -10 to -6 ‰. While one individual specimen may reflect a particular
437 history that appears in disequilibrium with the local river water, the analysis of small population ($n>10$) shows
438 that average values do reflect the characteristics of the river system. Molluscs from Main Himalayan rivers
439 consistently differ from the other environments surveyed (Ganga, foothills and Plain rivers) in that they have
440 lower $\delta^{18}\text{O}_{\text{Ara}}$ derived from the lower $\delta^{18}\text{O}_{\text{W}}$ of these rivers. In the floodplain, the type of watershed therefore
441 plays a significant role in the resulting shell isotopic signal. The difference between the two groups is about 2 ‰.
442 From the mollusc record of Surai khola Siwaliks, Dettman et al. (2001) derived an increase of river water $\delta^{18}\text{O}$
443 during the Mio-Pliocene compared to Middle Miocene. Such change from -12/-8 to -8/-6 ‰ may therefore
444 reflect a change in $\delta^{18}\text{O}$ of precipitation related to climatic evolution as well as a change in the river network.

445 We also investigated if seasonality information can be derived from the mollusc shells. While the
446 seasonal contrast for $\delta^{18}\text{O}$ of precipitation in one location can reach as high as 10 ‰ (as we reported for
447 Kathmandu), our record of different river systems shows that the rivers had a strong tendency to average this
448 contrast. Main Himalayan rivers show a small contrast of ~ 3 ‰, whereas small rivers originating in the

449 Himalayan foothills vary by 5 ‰ or more. This shows that, depending on the type of river where the mollusc
450 grows, the information in term of $\delta^{18}\text{O}$ amplitude can be different under identical climate conditions. A second
451 limitation is related to the recording by the mollusc itself. None of the specimen that we analysed showed pluri-
452 annual record that would allow deriving the whole amplitude of $\delta^{18}\text{O}$. This suggests that in the fossil record, the
453 application of such a tracer will require the analysis of a relatively large number of samples to provide the best
454 specimen. Extreme contrasts are recorded in isolated environments such as ponds. These cannot be used
455 quantitatively to trace past variations of precipitation as there is no control on the extent of evaporation. The
456 minimum $\delta^{18}\text{O}_{\text{Ara}}$ certainly documents the wet season as stated by Dettman et al. (2001) but it is difficult to know
457 how such system is related to the river environment. We suggest therefore that samples that do not present
458 extreme values due to evaporation should be preferred when possible, in order to be sure to trace rivers and not
459 closed bodies of water or ponds.

460 Finally, the carbon isotope composition of shells is controlled by that of DIC and, for a significant
461 proportion, by carbon derived from metabolic processes. The resulting $\delta^{13}\text{C}$ of shells is 2-3‰ lower than
462 predicted by inorganic equilibrium with DIC. Shell aragonite has therefore the potential to trace processes that
463 control the $\delta^{13}\text{C}$ of DIC in river water. The evolution of the flora from C_3 to C_4 during the Mio-Pliocene that
464 affect the whole Gangetic basin (e.g. Quade et al, 1995) is of course a major event that can be traced. In addition
465 this should increase the $\delta^{13}\text{C}$ of land derived organic carbon and likely that of phytoplankton. DIC is also
466 controlled by lithologies that are weathered in the watershed and changes in the proportion of carbonate to
467 silicate weathering ratio in the Himalaya should also be detectable. Singh et al. (in press) reported $\delta^{13}\text{C}_{\text{DIC}}$ for the
468 Brahmaputra and Himalayan tributaries that are 3 to 5 ‰ lower than those of the Ganga or Main Himalayan
469 rivers draining Nepal. This simply reflects the fact that less carbonate rocks are exposed to erosion in Eastern
470 Himalaya. $\delta^{13}\text{C}$ of shells in the Siwaliks record have therefore the potential to trace long term variation of the
471 occurrence of carbonate rocks in the river drainage.

472 Studies of fossil shells in the sedimentary record have the potential to document river water evolution.
473 One option is to rely on bulk compositions avoiding abnormally high $\delta^{18}\text{O}$ values that are clearly related to
474 evaporation. It requires also a statistical approach in order to determine average compositions. Because
475 watershed characteristics control part of the isotopic composition of the shell, efforts should be made to derive
476 river type from complementary sedimentological and geochemical characteristics. The second approach relies on
477 the analysis of intra-shell variations. It has clearly the potential to document the intensity of the seasonal contrast

478 provided the river environment has been determined. In this case again, the sedimentological context is essential
479 to derive climatological implications.

480 **Acknowledgements**

481 This research was funded by the ECLIPSE Centre National de la Recherche Scientifique program. The first
482 author is grateful to the French Minister of foreign affairs (MAE) and French Embassy in Kathmandu for
483 providing scholarship to complete his doctorate degree in France. Dr. Sunil K. Singh (from PRL Ahmadabad) is
484 warmly thanked for his continuous support and expertise during sampling in the Gangetic plain. We thank David
485 Dettman and an anonymous reviewer for their very careful and helpful comments.

487 **References**

- 488 Abell, P.I., 1985. Oxygen isotope ratios in modern African gastropod shells: a database for paleoclimatology.
489 Chem. Geol. (Isot.Geosci.Sect.) 58, 183–193.
- 490 Aucour, A.M., France-Lanord, C., Pedoja, K., Pierson-Wickmann, A.C. and Sheppard S.M.F. Fluxes and sources
491 of particulate organic carbon in the Ganga-Brahmaputra river system. Global Biogeochemical Cycle, in
492 press.
- 493 Aucour, A.M., Sheppard, S.M.F. and Savoye, R., 2003. $\delta^{13}\text{C}$ of fluvial mollusk shells (Rhône River): A proxy
494 for dissolved inorganic carbon? Limnol. Oceanogr. 48, 2186-2193.
- 495 Bhattacharya, S.K., Gupta, S.K. and Krishnamurthy, R.V., 1985. Oxygen and hydrogen isotopic ratios in
496 groundwaters and river waters from India. Proc. Indian Acad. Sci. (Earth Planet. Sci.) 94(3), 283-295.
- 497 Bhattacharya, S.K., Froehlich, K., Aggarwal, P.K. and Kulkarni, K.M., 2003. Isotopic variation in Indian
498 Monsoon precipitation: Records from Bombay and New Delhi. Geophysical Research Letters 30(24),
499 11(1)-11(4).
- 500 Dettman, D.R., Matthew, J.K., Quade, J., Ryerson, F.J., Ojha, T.P. and Hamidullah, S., 2001. Seasonal stable
501 isotope evidence for a strong Asian monsoon throughout the past 10.7 m.y. Geology 29(1), 31-34.
- 502 Dettman, D.L., Reische, A.K. and Lohmann, C.K., 1999. Controls on the stable isotope composition of seasonal
503 growth bands in aragonitic fresh-water bivalve (unionidae). Geochim. Cosmochim. Acta 63 1049-1057.
- 504 Deuser, W.G. and Degens, E.T., 1967. Carbon isotope fractionation in the system $\text{CO}_2(\text{gas}) - \text{CO}_2(\text{aqueous}) -$
505 $\text{HCO}_3^-(\text{aqueous})$. Nature 215, 1033-1035.
- 506 DHM, 1998. Hydrological records of Nepal. Ministry of Water Resources, Department of Hydrology and
507 Meteorology, Kathmandu, Nepal, 264 p.
- 508 DHM, 2002. Precipitation Records of Nepal. Ministry of Water Resources, Department of Hydrology and
509 Meteorology, Kathmandu, Nepal.

- 510 Epstein, S. and Mayeda, T., 1953. Variation of $\delta^{18}\text{O}$ content in waters from natural sources. *Geochim.*
511 *Cosmochim. Acta* 4, 213–214.
- 512 Epstein, S., Buchsbaum, R., Lowenstam, H. and Urey, H.C., 1953. Revised carbonate–water isotopic
513 temperature scale. *Geol. Soc. Am. Bull.* 64, 1315-1326.
- 514 Evans, M.J., Derry, L.A. and France-Lanord, C., 2004. Geothermal fluxes of alkalinity in the Narayani river
515 system of central Nepal. *Geochemistry, Geophysics and Geosystems* 5(8), 1-21.
- 516 Fritz, P., and Poplawski, S., 1974. ^{18}O and ^{13}C in the shells of freshwater mollusks and their environment. *Earth*
517 *Planet. Sci. Lett.* 24, 91–98.
- 518 Gajurel, A.P., France-Lanord, C. and Huyghe, P., 2003. Compositions isotopiques (carbone et oxygène) de
519 gastéropodes et bivalves des Siwaliks: Implications paleo- environnementales sur le system himalayen
520 depuis le Miocène. *TectoClim, UMR USTL-CNRS, Lille*, p. 25.
- 521 Galy, A. and France-Lanord, C., 1999. Weathering processes of the in the Ganges-Brahmaputra basin and the
522 riverine alkalinity budget. *Chem. Geol.* 159, 31-60.
- 523 Garzione, C.N, Dettman, D.L., Quade, J., DeCelles, P.G. and Butler, R.F., 2000a. High time on the Tibetan
524 Plateau: Paleoelevation of the Thakkhola graben, Nepal. *Geology* 28(4), 339-342.
- 525 Garzione, C.N, Quade, J., DeCelles, P.G. and English, N.B., 2000b. Predicting palaeoelevation of Tibet and the
526 Himalaya from $\delta^{18}\text{O}$ vs. altitude gradients in meteoric waters across the Nepal Himalaya. *Earth Plan.*
527 *Sci. Lett.* 183, 215–229.
- 528 Grossman, E.L., and Ku, T.-L., 1986. Oxygen and carbon isotope fractionation in biogenic aragonite:
529 temperature effects. *Chem. Geol., Isot. Geosci. Sect.* 59, 59 – 74.
- 530 Gupta, S., 1997. Himalayan drainage patterns and the origin of fluvial megafans in the Ganges foreland basin.
531 *Geology* 25, 11-14.
- 532 Hagen, T., 1969. Reports of the Geological Survey of Nepal. *Denkschrift der Schweizerischen Naturforschenden*
533 *Gesellschaft* 1, 185 p.
- 534 Jenkins, D.T., Sharma, C.K. and Hassett, J.M., 1987. A stable isotope reconnaissance of groundwater resources
535 in the Kathmandu Valley, Nepal. *Proceedings of an International Symposium on the use of isotope*
536 *techniques in water resources development organization, IAEA -SM-299/119P, 775-778.*
- 537 Kaandorp, R.J.G., Vonhof, H.B., Busto, C.D., Wesselingh, F.P., Ganssen, G.M., Marmól, A.E., Pittman, L.R.
538 and van Hinte, J.E., 2003. Seasonal stable isotope variations of the modern Amazonian freshwater
539 bivalve *Anodontites trapesialis*. *Palaeo geogr. Palaeoclimatol. Palaeoecol.* 194, 339-354.

- 540 Klein, R.T., Lohmann, K.C. and Thayer, C.W., 1996. Sr/Ca and $^{13}\text{C}/^{12}\text{C}$ ratios in skeletal calcite of *Mytilus*
541 *trossulus*: Covariation with metabolic rate, salinity, and carbon isotopic composition of seawater.
542 *Geochim. Cosmochim. Acta* 60(21), 4207-4221.
- 543 Kim, S.T and O'Neil, J.R., 1997. Equilibrium and nonequilibrium oxygen isotope effects in synthetic carbonates.
544 *Geochim. Cosmochim. Acta* 61(16), 3461-3475.
- 545 Krishnamurthy, R.V. and Bhattacharya, S.K., 1991. Stable oxygen and hydrogen isotope ratios in shallow
546 ground waters from India and a study of the role of evapotranspiration in the Indian monsoon. In
547 Taylor, H., O'Neil, J. and Kaplan, I., (eds.), *Isotope Geochemistry: a Tribute to Samuel Epstein*.
548 *Geochemical Society: Texas, Special Publication*, 187–193.
- 549 Lécuyer, C., Reynard, B. and Martineau, F., 2004. Stable isotope fractionation between mollusc shells and
550 marine waters from Martinique Island. *Chem. Geol.* 213(4), 293-305.
- 551 Lowenstam, A. and Epstein, S., 1954. Paleotemperatures of the Post-Aptian Cretaceous as determined by the
552 oxygen isotope method. *J. Geol.* 62, 207 – 248.
- 553 Margosian, A., Tan, F.C., Cai, D., and Mann, K.H., 1987. Sea-water temperature records from stable isotope
554 profiles in the shell of *Modiolus modiolus*. *Estuar. Coast. Shelf Sci.* 25, 81 – 89.
- 555 McCrea, J.M., 1950. On the isotopic chemistry of carbonates and a paleotemperature scale. *J. Chem. Phys.* 18,
556 849-857.
- 557 Michener, R.H. and Shell, D.M., 1994. Stable isotope ratios as tracers in marine aquatic food webs. In: Lajtha, K.
558 and Michener, R.H. (eds), *Stable Isotopes in Ecology and Environmental Studies*. Blackwell Scientific
559 Publications, 138–157.
- 560 Miller, K.G., Fairbanks, R.G., and Mountain, G.S., 1987. Tertiary oxygen isotope synthesis, sea level history,
561 and continental margin erosion. *Paleoceanography* 2, 1 – 19.
- 562 Neseemann, H., Korniuschin, A., Khanal, S. and Sharma, S., 2001. Molluscs of the families Sphaeriidae and
563 Corbiculidae (*Bivalvia*, *Veneroidea*) of Nepal (Himalayan midmountains and terai), their anatomy and
564 affinities. *Acta Conchyliorum, Wien und Ludwigsburg* 4, 1-33.
- 565 Quade, J., Cater, J.M.L., Ojha, T.P., Adam, J. and Harrison, T.M., 1995. Late Miocene environmental change in
566 Nepal and the northern Indian subcontinent: Stable isotopic evidence from paleosols. *Geol. Soc. Am.*
567 *Bull.* 107, 1381-1397.
- 568 Ramesh, R. and Sarin, M.M., 1992. Stable isotope study of the Ganga (Ganges) river system. *Jour. Hydrol.* 139,
569 49–62.

- 570 Romanek, S.C., Grossman, E.L. and Morse, W.J., 1992. Carbon isotopic fractionations in synthetic aragonite and
571 calcite: effects of temperature and precipitation rate. *Geochim. Cosmochim. Acta* 56, 419-430.
- 572 Rao, K.L., 1979. *India's water wealth*. Orient Longman limited, New Delhi, 267 pp.
- 573 Rozanski, K., Araguas-Araguas, L., and Gonfiantini, R., 1993. Isotopic patterns in modern global precipitation.
574 In: Swart, P., Lohmann, K.C., McKenzie, J. and Savin, S. (eds), *Climate Change in Continental Isotope*
575 *Records*. Am. Geophys. Union Monogr. 78, 1-36.
- 576 Rubinson, M. and Clayton, R.N., 1969. Carbon-13 fractionation between aragonite and water. *Geochim.*
577 *Cosmochim. Acta* 33, 997-1002.
- 578 Seeber, L. and Gornitz, V., 1983. River profiles along the Himalayan arc as indicators of active tectonics.
579 *Tectonophysics* 92, 335-367.
- 580 Shackleton, N.J., 1986. Paleogene stable isotope events. *Palaeo geogr. Palaeoclimatol. Palaeoecol.* 57, 91 – 102.
- 581 Sharma, S., Joachimski, M., Sharma, M., Tobschall, H.J., Singh, I.B., Sharma, C., Chauhan, M.S. and
582 Morgenroth, G., 2004. Late Glacial and Holocene environmental changes in Ganga plain, northern
583 India. *Quat. Sci. Rev.* 23, 139 – 153.
- 584 Siegel, D.I. and Jenkins, D.T., 1987. Isotope analysis of groundwater flow systems in a wet alluvial fan, southern
585 Nepal. *Proceedings of an International Symposium on the use of isotope techniques in water resources*
586 *development organization IAEA -SM-299/118*, 475-482.
- 587 Singh, S.K., Sarin, M.M. and France-Lanord, C., in press. Chemical Erosion in the Eastern Himalaya: Major ion
588 composition of the Brahmaputra and $\delta^{13}\text{C}$ of dissolved inorganic carbon. *Geochem. Cosmochem. Acta*.
- 589 Sinha, R. and Friend, P.F., 1994. River systems and their sediment flux, Indo-Gangetic plains, Northern Bihar,
590 India. *Sedimentology* 41, 825-845.
- 591 Subba Rao, N.V., 1989. *Handbook of freshwater mollusks of India*. pub. Zool. Sur. India, Calcutta, 289 P.
- 592 Subba, B.R. and Ghosh, T.P., 2000. Some freshwater mollusks from eastern and central Nepal. *J. Bombay Nat.*
593 *His. Soc.* 97(3), 452-455.
- 594 Weidman, C.R., Jones, G.A., and Lohmann, K.C., 1994. The long-lived mollusk *Arctica islandica*: a new
595 paleoceanographic tool for the reconstruction of bottom temperatures for the continental shelves of the
596 North Atlantic Ocean. *J. Geophys. Res.* 99, 18305 – 18314.
- 597 Wells, N.A., and Dorr, Jr.J.A., 1987. Shifting of the Kosi River, northern India. *Geology* 15, 204-207.
- 598 Woodruff, F., Savin, S., and Douglas, R.G., 1981. Miocene stable isotope record: a detailed deep Pacific Ocean
599 study and its paleoclimatic implications. *Science* 212, 665 – 668.

600

601

602

603 **Figure captions**

604

605 **Figure 1:** Sample location along the Main Ganga River, Main Himalayan rivers, plain river, in lakes and ponds
606 in Ganga plain and mountain area.

607

608 **Figure 2:** Photomicrographs of some collected fauna. The scale bar is 1 cm

609

610 **Figure 3:** $\delta^{18}\text{O}_\text{W}$ values of water samples as a function of: **(3a)** sampling elevation for the High Himalayan
611 rivers, Kathmandu Valley rivers, foothills and Main Himalayan rivers and Phewa Lake, and **(3b)** longitude for
612 the Main Ganga stream in the Ganga plain.

613

614 **Figure 4:** Histograms showing $\delta^{18}\text{O}_\text{W}$ values of rivers and pond waters for monsoon (June to September) and dry
615 seasons (above) and $\delta^{18}\text{O}_\text{Ara}$ values of mollusc shells sampled in these respective water environments (below).

616

617 **Figure 5:** Day to day record of $\delta^{18}\text{O}$ values of rain water in Kathmandu (Nepal) during the year 2001-02. O and
618 H isotopic compositions are listed in appendix 3. Filled circles correspond to measured $\delta^{18}\text{O}$ data. Open dots
619 correspond to calculated $\delta^{18}\text{O}$ values from measured δD data using our determination of local meteoric water line
620 $\delta\text{D} = 8.10 \delta^{18}\text{O} + 12.3$ (Fig. 6).

621

622 **Figure 6:** δD vs. $\delta^{18}\text{O}$ plot for river water samples listed in table 2. MWL represents the global meteoric water
623 line ($\delta\text{D} = 8\delta^{18}\text{O} + 10$). Samples include river data from Jenkins et al., (1987); Ramesh and Sarin, (1992);
624 Garzzone et al., (2000b).

625

626 **Figure 7:** Histograms showing $\delta^{13}\text{C}_\text{DIC}$ values of river waters for foothills rivers, Main Himalayan rivers and the
627 Main Ganga River (above) and $\delta^{13}\text{C}_\text{Ara}$ values of mollusc shells sampled from these respective water
628 environments (below). Arrows indicate average $\delta^{13}\text{C}_\text{DIC}$ and $\delta^{13}\text{C}_\text{Ara}$ values.

629

630 **Figure 8:** $\delta^{13}\text{C}_\text{DIC}$ vs. longitude for the Main Ganga stream in the Ganga plain.

631

632 **Figure 9:** Ontogenic evolution of C and O stable isotopes for the shell of *Bellamyia Bengalensis* (BR 316-10)
633 sampled from eastern Main Ganga River.

634

635 **Figure 10a:** Ontogenic evolution of C and O stable isotopes for the shell of *Bellamyia Bengalensis* (BR 337-3)
636 sampled from the Ghaghara (Narayani) and for the shell of *Brotia* sp. (Chit 1) from the Rapti River.

637

638 **Figure 10b** Ontogenic evolution of C and O stable isotopes for the shell of *Corbicula* sp. (Btw-2 cor) sampled
639 from the Tinau Khola.

640

641 **Figure 11:** Calculated $\delta^{18}\text{O}_{\text{Ara}}$ derived from river water compositions and temperature condition for different
642 river water environments and seasons. The calculation assumes isotopic equilibrium with water and aragonite-
643 water fractionation of Dettman et al (1999).

644

645 **Figure 12:** Plot of $\delta^{18}\text{O}_{\text{Ara}}$ shell's average value vs. $\delta^{18}\text{O}_{\text{W}}$ water's average value for foothills rivers, Main
646 Himalayan rivers, plain rivers and the Main Ganga River. Theoretical ambient temperature lines are drawn
647 according to the fractionation equation of Grossman and Ku (1986) modified by Dettman et al. (1999). The
648 average values for waters ($\delta^{18}\text{O}_{\text{W}}$) and shells ($\delta^{18}\text{O}_{\text{Ara}}$) are calculated using the data of tables 2 and 3 respectively,
649 for each setting.

650

651 **Figure 13:** Plot of $\delta^{13}\text{C}_{\text{Ara}}$ shell's average value vs. $\delta^{13}\text{C}_{\text{DIC}}$ water's average value for foothills rivers, Main
652 Himalayan rivers, plain rivers and the Main Ganga River. The average values for waters ($\delta^{13}\text{C}_{\text{DIC}}$) and shells
653 ($\delta^{18}\text{O}_{\text{Ara}}$) are calculated using the data of tables 2 and 3 respectively, for each setting.

654

655 **Table captions**

656

657 **Table 1a.** Bulk shell $\delta^{18}\text{O}$ and $\delta^{13}\text{C}$ data for three different treatments of the same specimen *Bellamya*
658 *bengalensis* (Bakai KR1).

659 **Table 1b.** $\delta^{18}\text{O}$ and $\delta^{13}\text{C}$ data for standard aragonite Maroc IKON.

660 **Table 2.** Hydrogen, oxygen and carbon isotopic data for rivers and pond waters from North Himalaya, foothills,
661 and Ganga plain with sampling elevation and physical properties of waters.

662 **Table 3.** Oxygen and carbon isotopic data for the modern mollusc shells from North Himalaya, Phewa Lake,
663 foothills rivers, rivers in the Ganga plain and ponds with sampling elevation.

664 **Table 4.** Intra-shell $\delta^{18}\text{O}$ and $\delta^{13}\text{C}$ data for modern freshwater mollusc shells from foothills rivers, Main
665 Himalayan rivers and Main Ganga River.

666 **Appendix 1.** Location of river and pond water samples in Himalaya and Ganga plain.

667 **Appendix 2.** Location of modern shell samples collected from rivers and ponds.

668 **Appendix 3.** Hydrogen and oxygen isotopic data of the meteoric waters collected between 2001 and 2002 at
669 Subidhanagar in Kathmandu (27° 41' 6"; 85° 20' 59" and 1300 m).

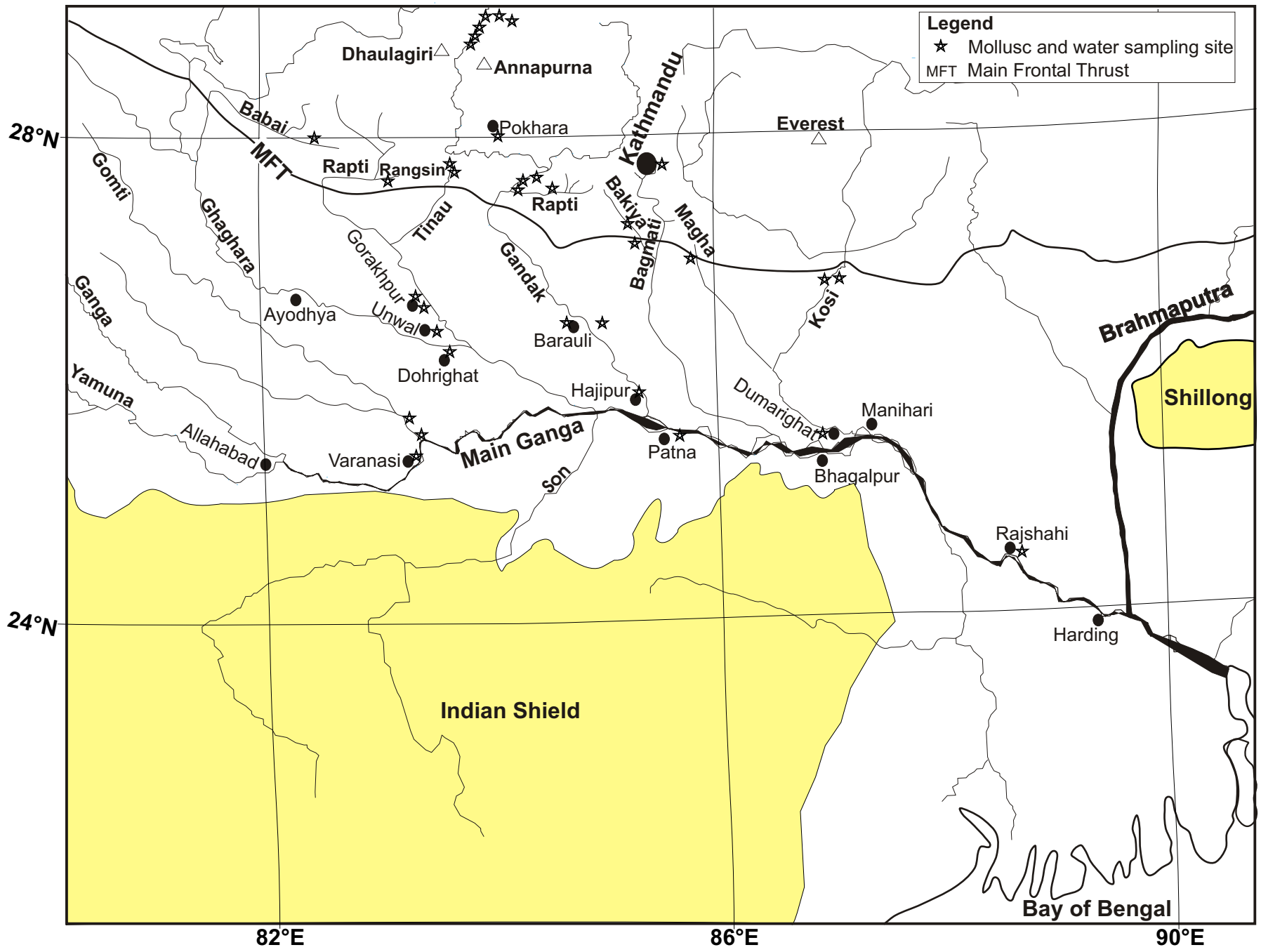
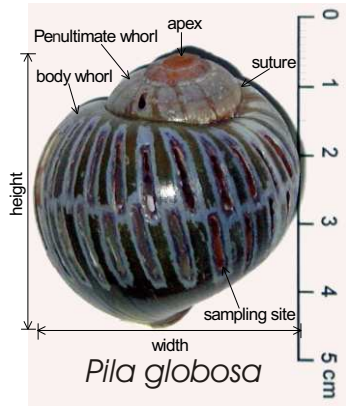


Fig.1 Gajurel et al.



Bellamyia bengalensis



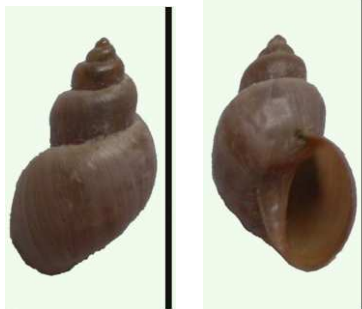
Bithynia sp.



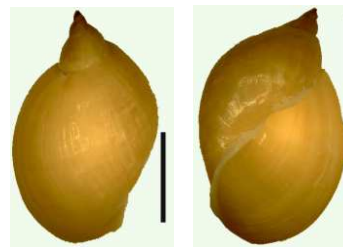
Melanoide cf. *Tuberculata*



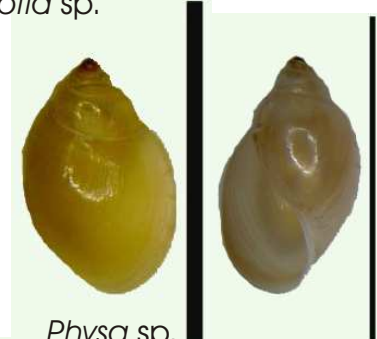
Brotia sp.



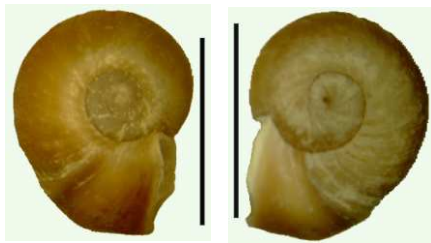
Lymnaeinae sp.



Lymnaea acuminata



Physa sp.



Indoplanorbis exustus



Gyraulus sp.



Lamellidens sp.



Corbicula sp.



Fig.2 Gajurel et al.

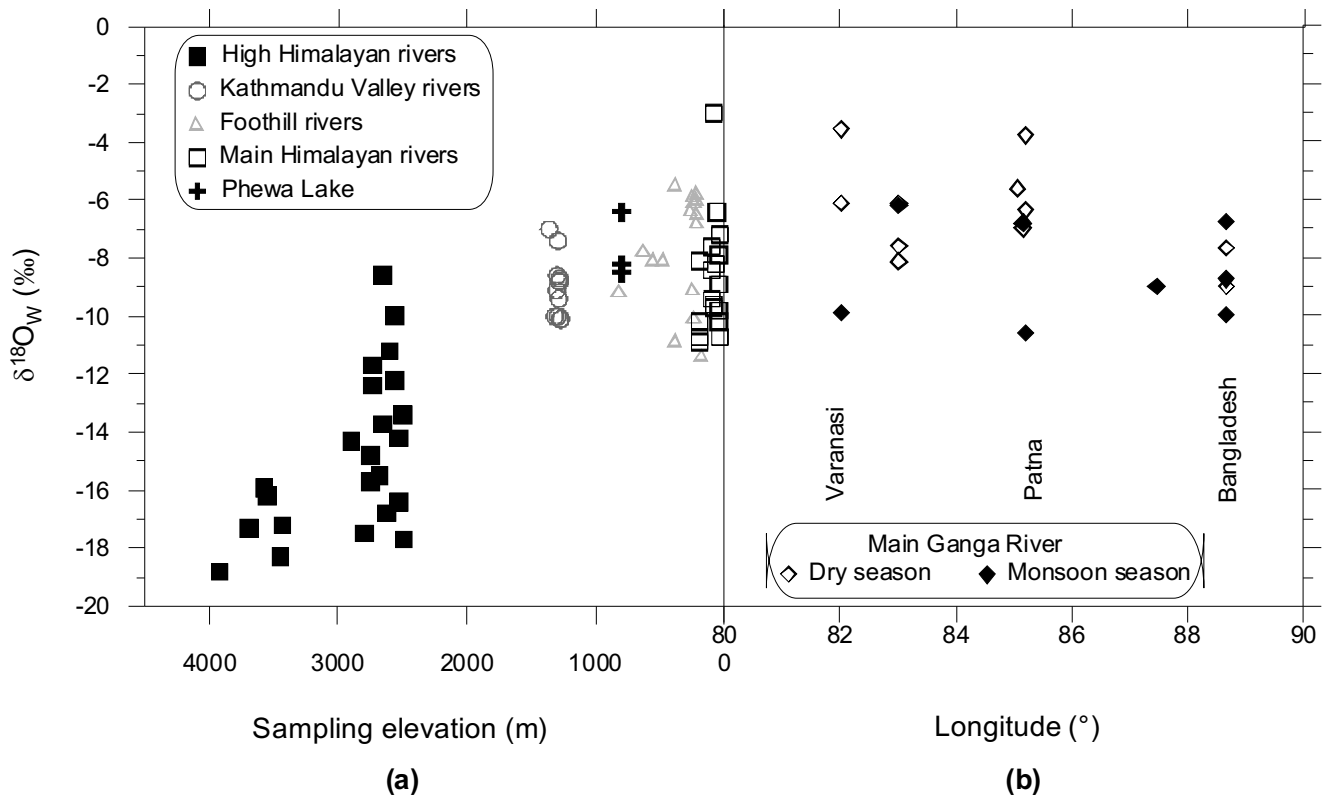


Fig 3 Gajurel et al.

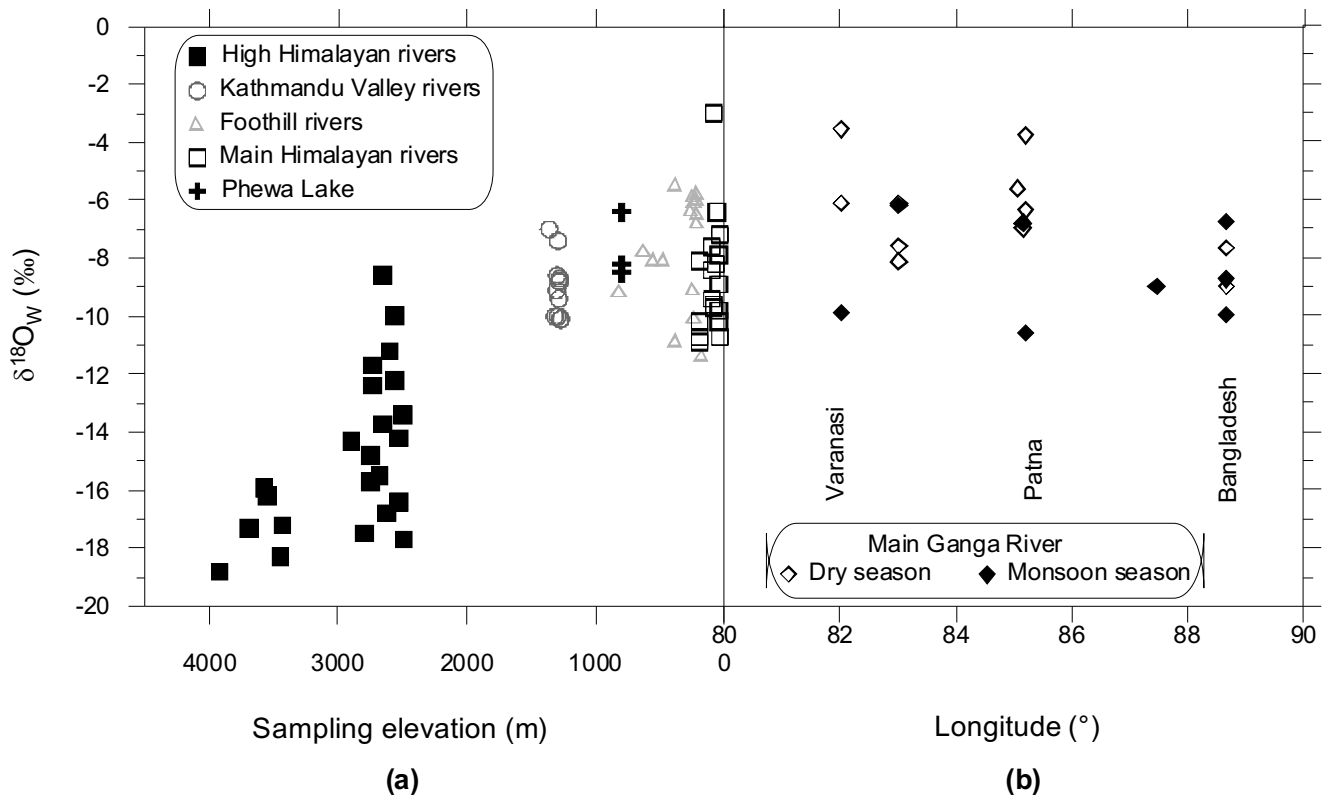


Fig 3 Gajurel et al.

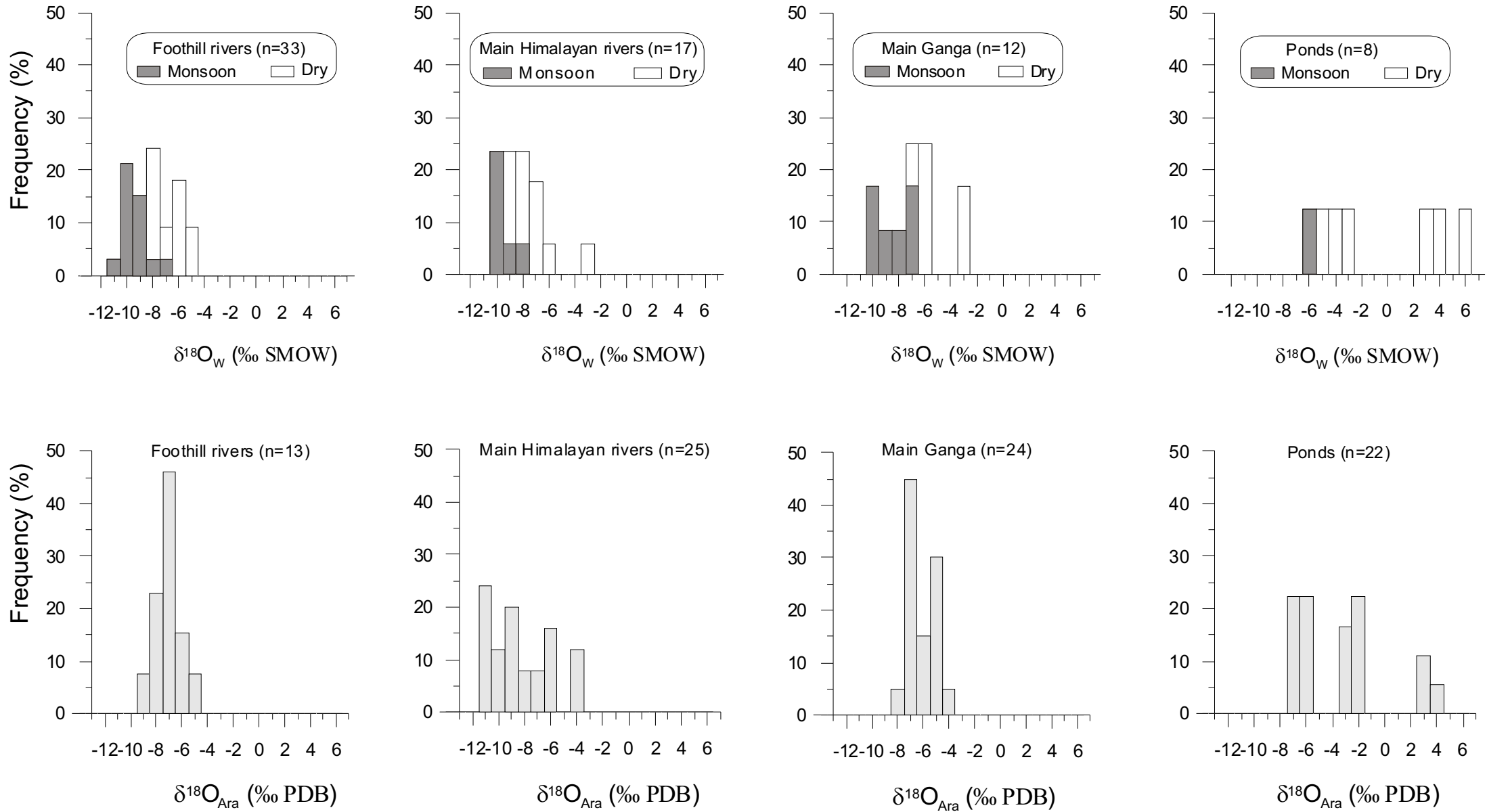


Fig. 4 Gajurel et al.

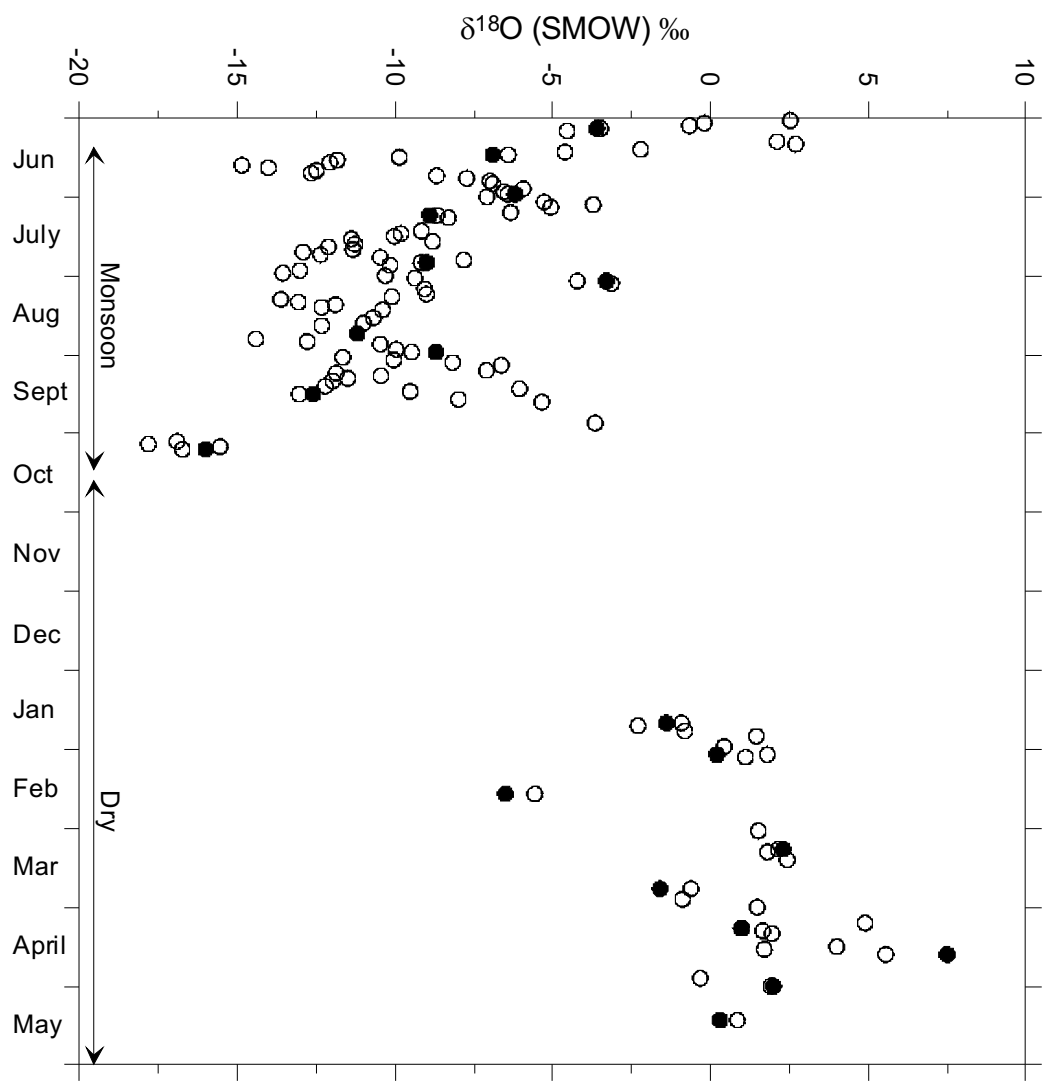


Fig 5 Gajurel et al.

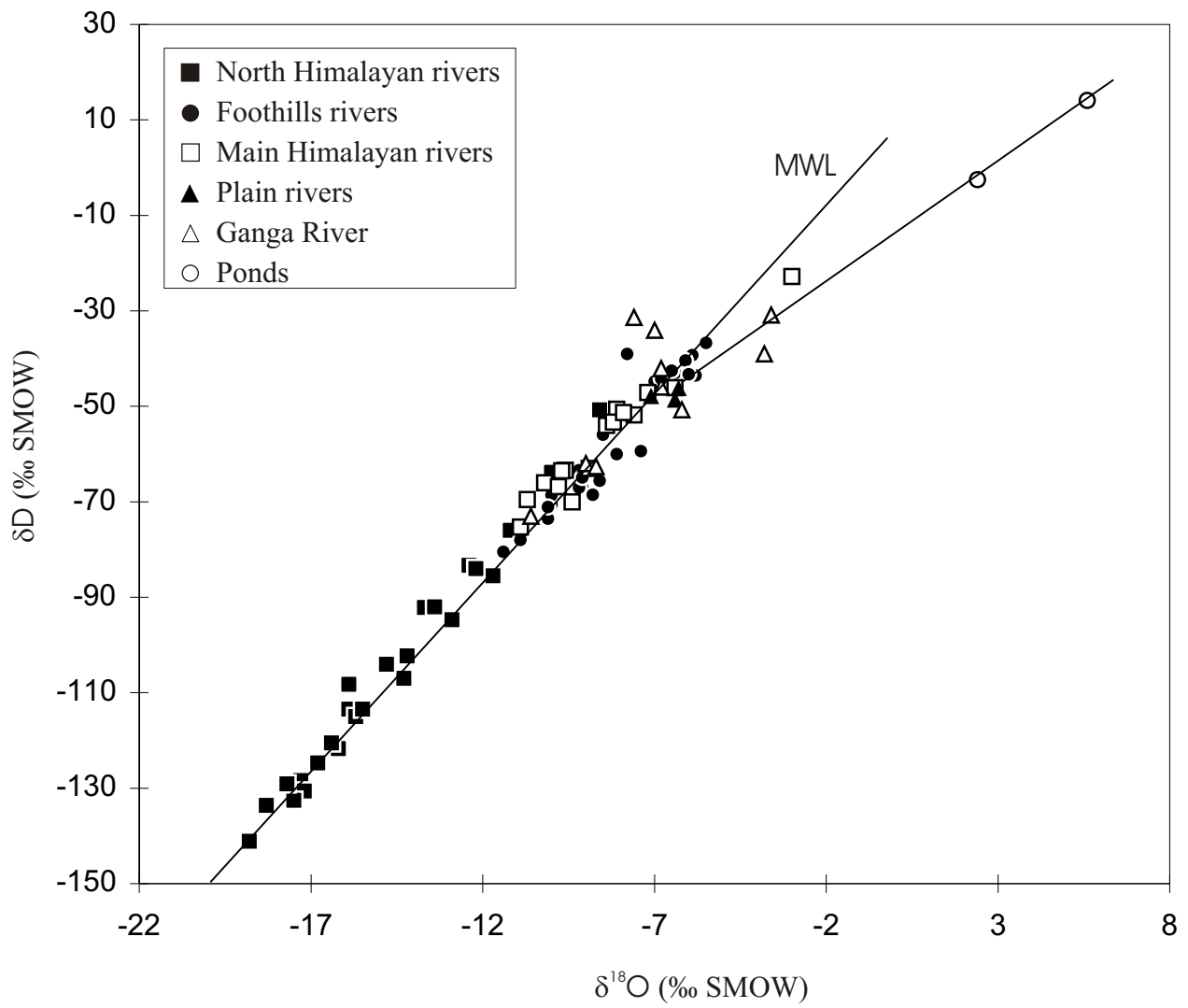


Fig6 Gajurel et al.

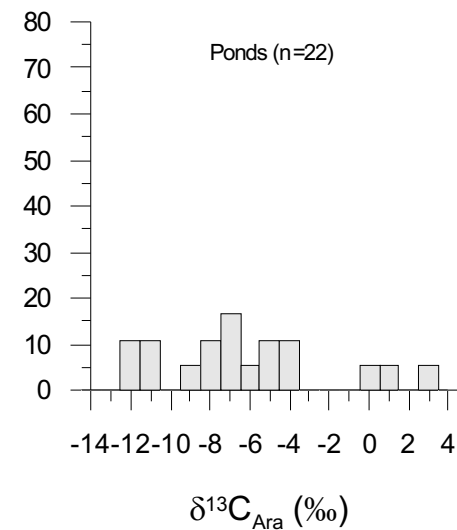
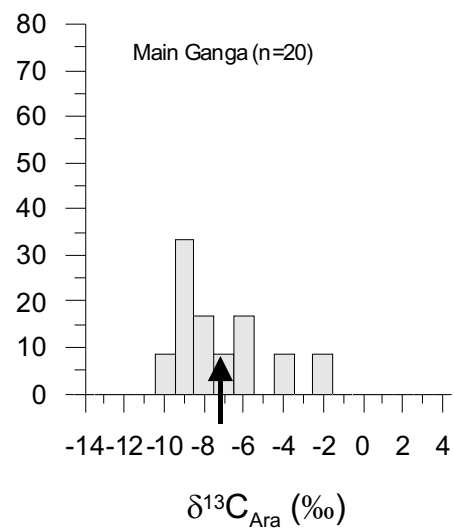
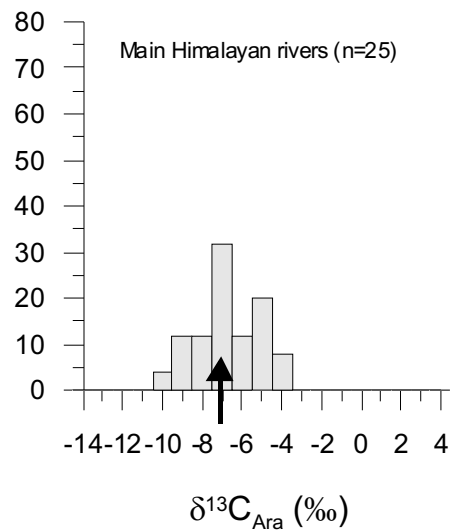
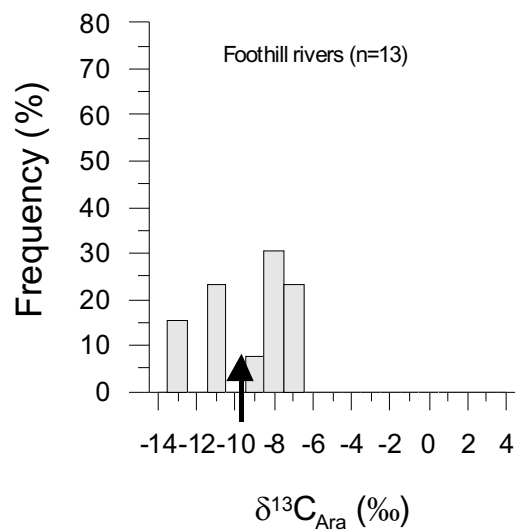
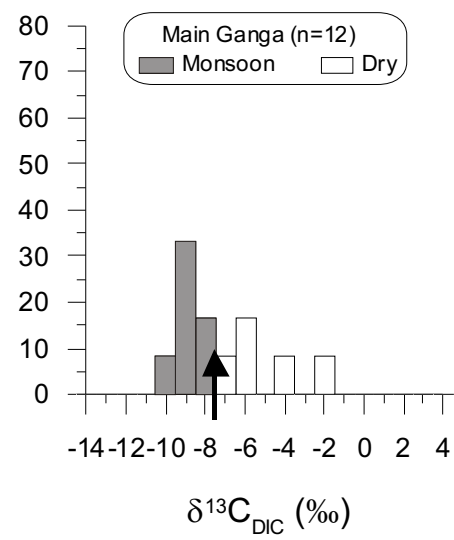
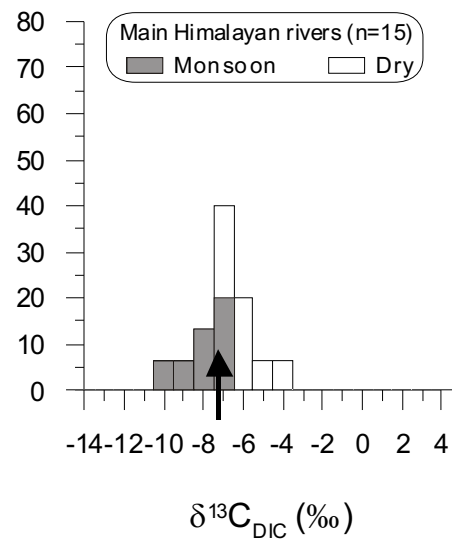
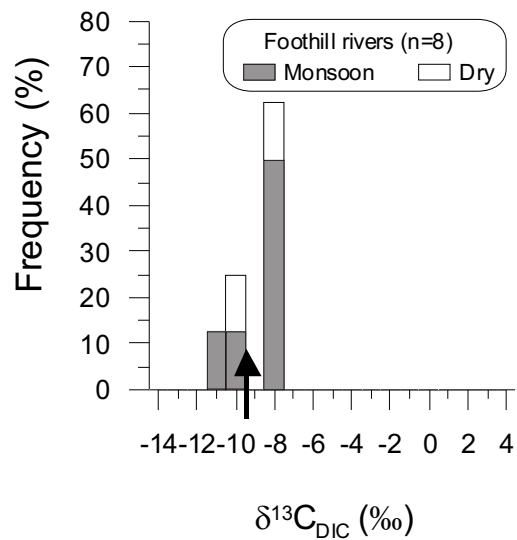


Fig 7 Gajurel et al.

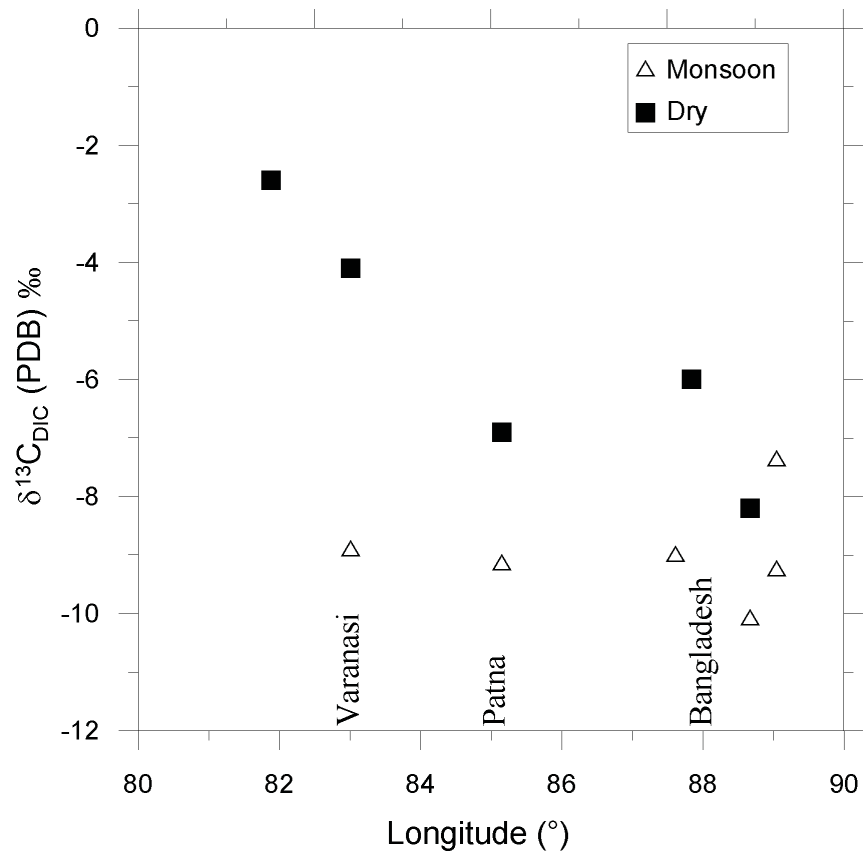


Fig. 8 Gajurel et al.

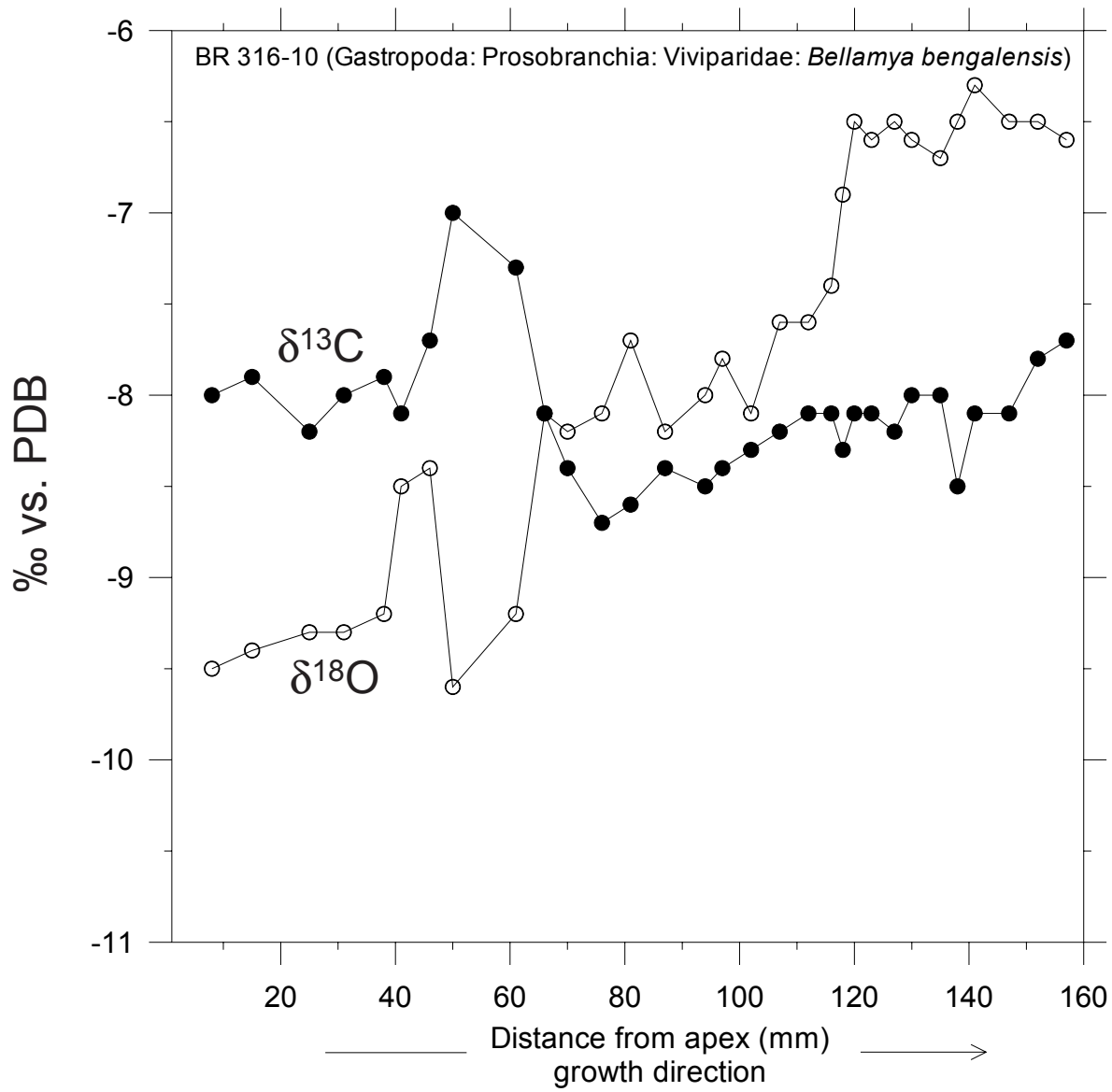


Fig 9 Gajurel et al.

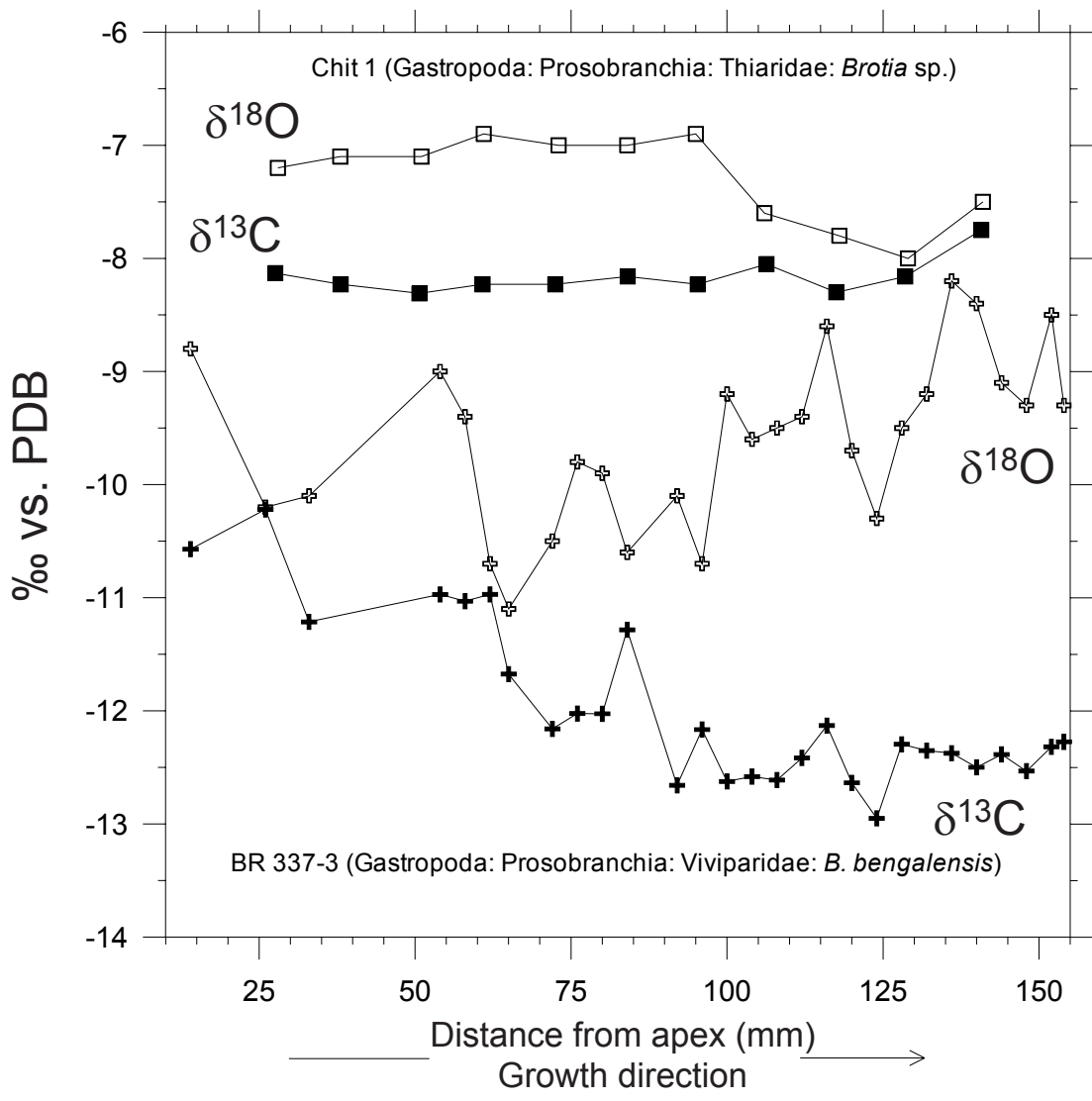


Fig 10a Gajurel et al.

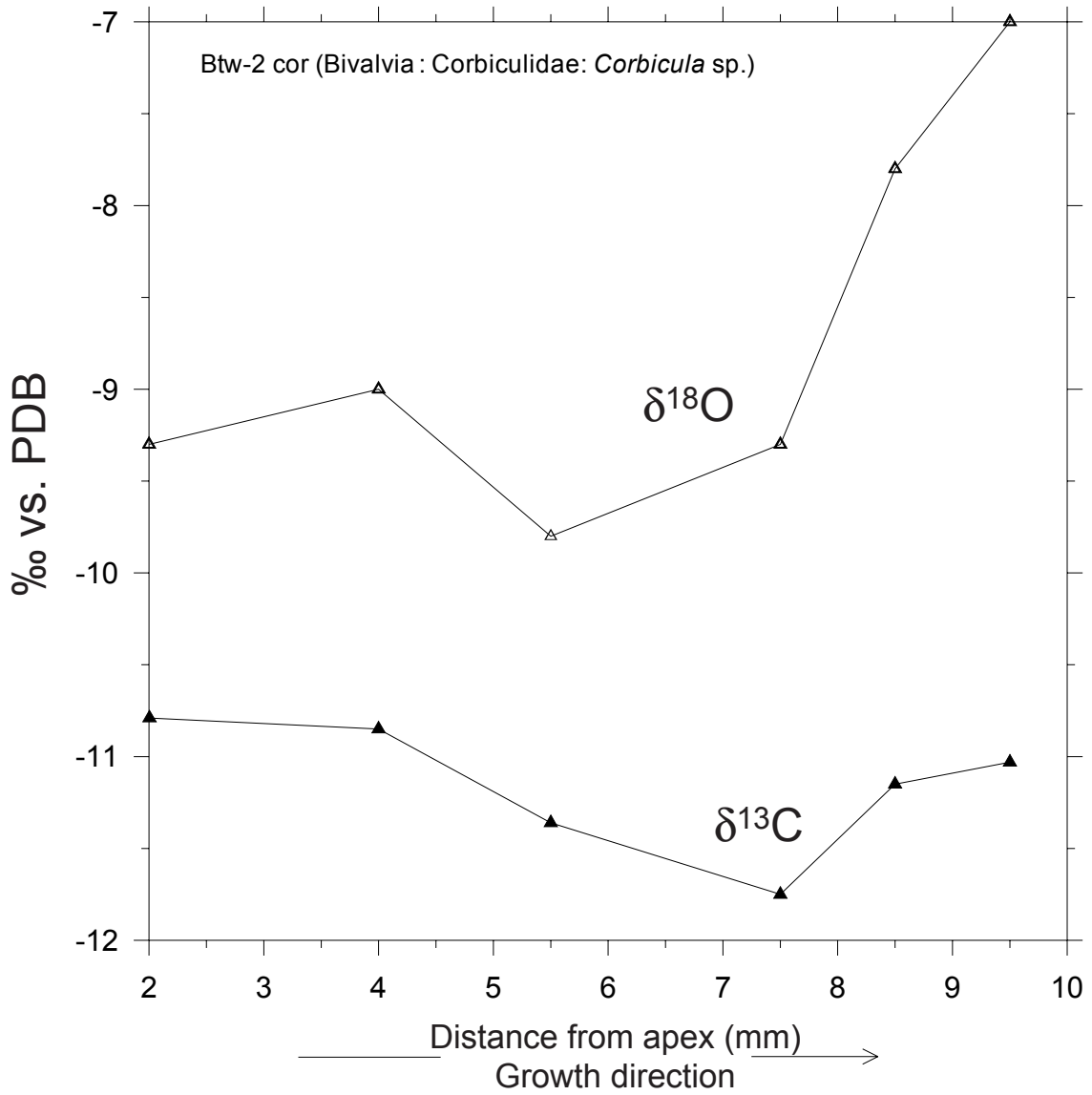


Fig 10b Gajurel et al.

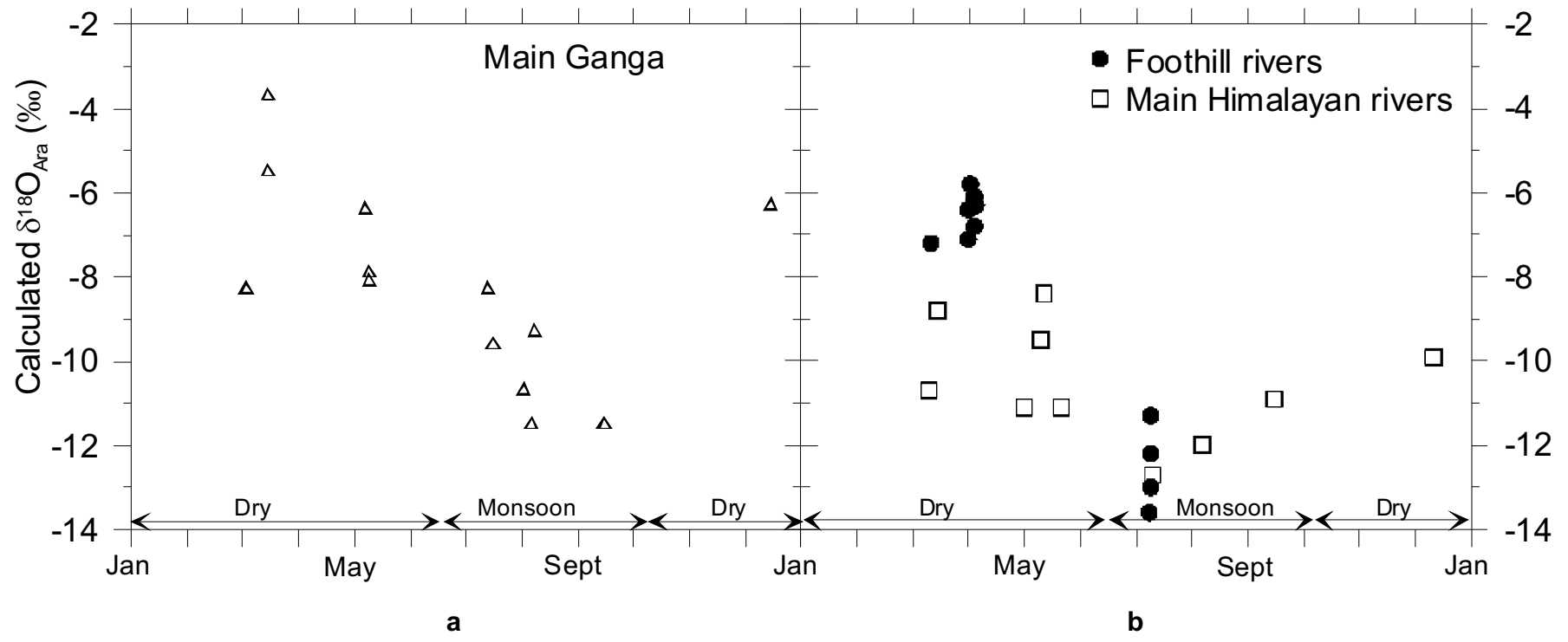


Fig 11 Gajurel et al.

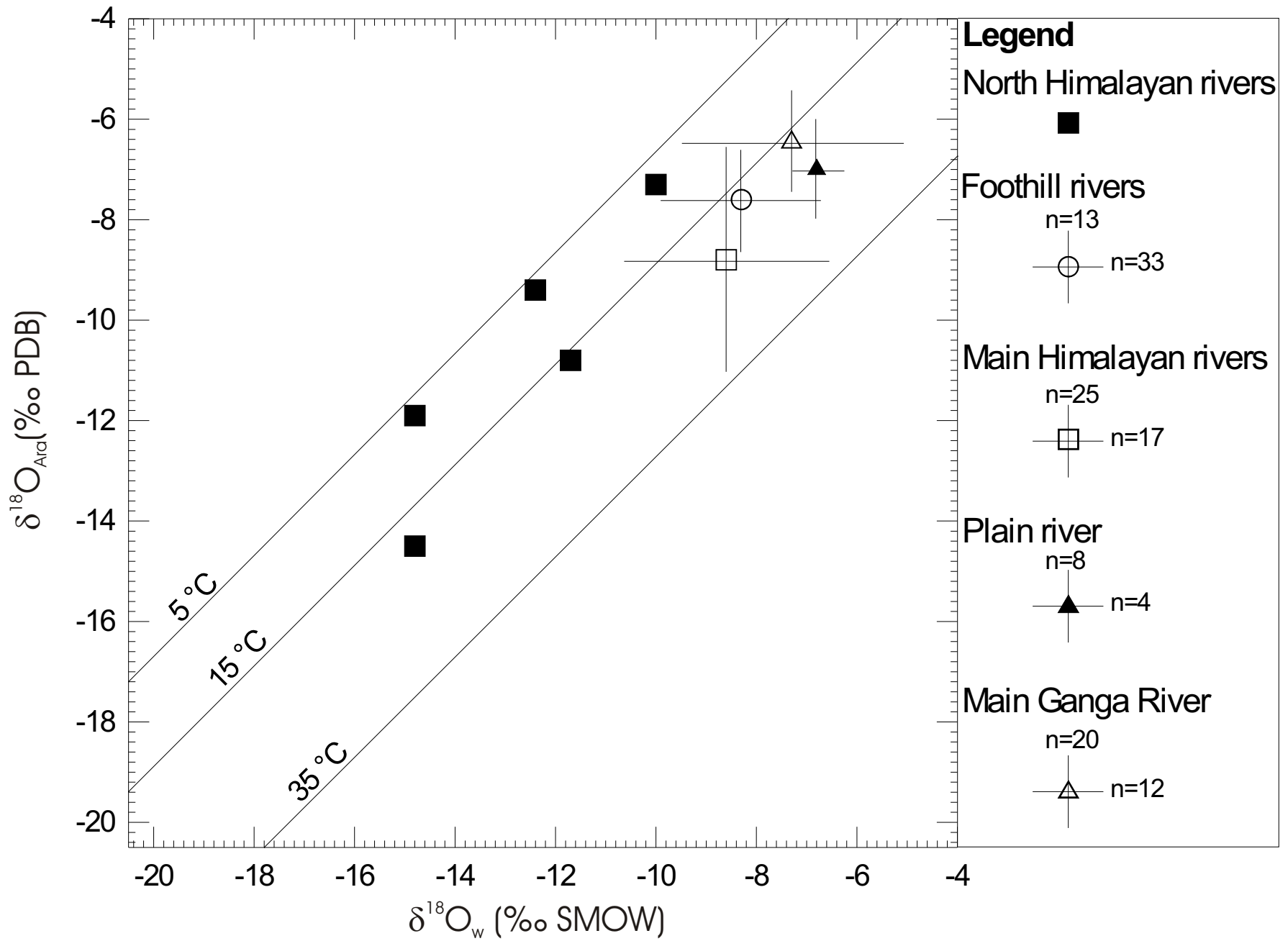


Fig.12 Edited Gajurel et al.

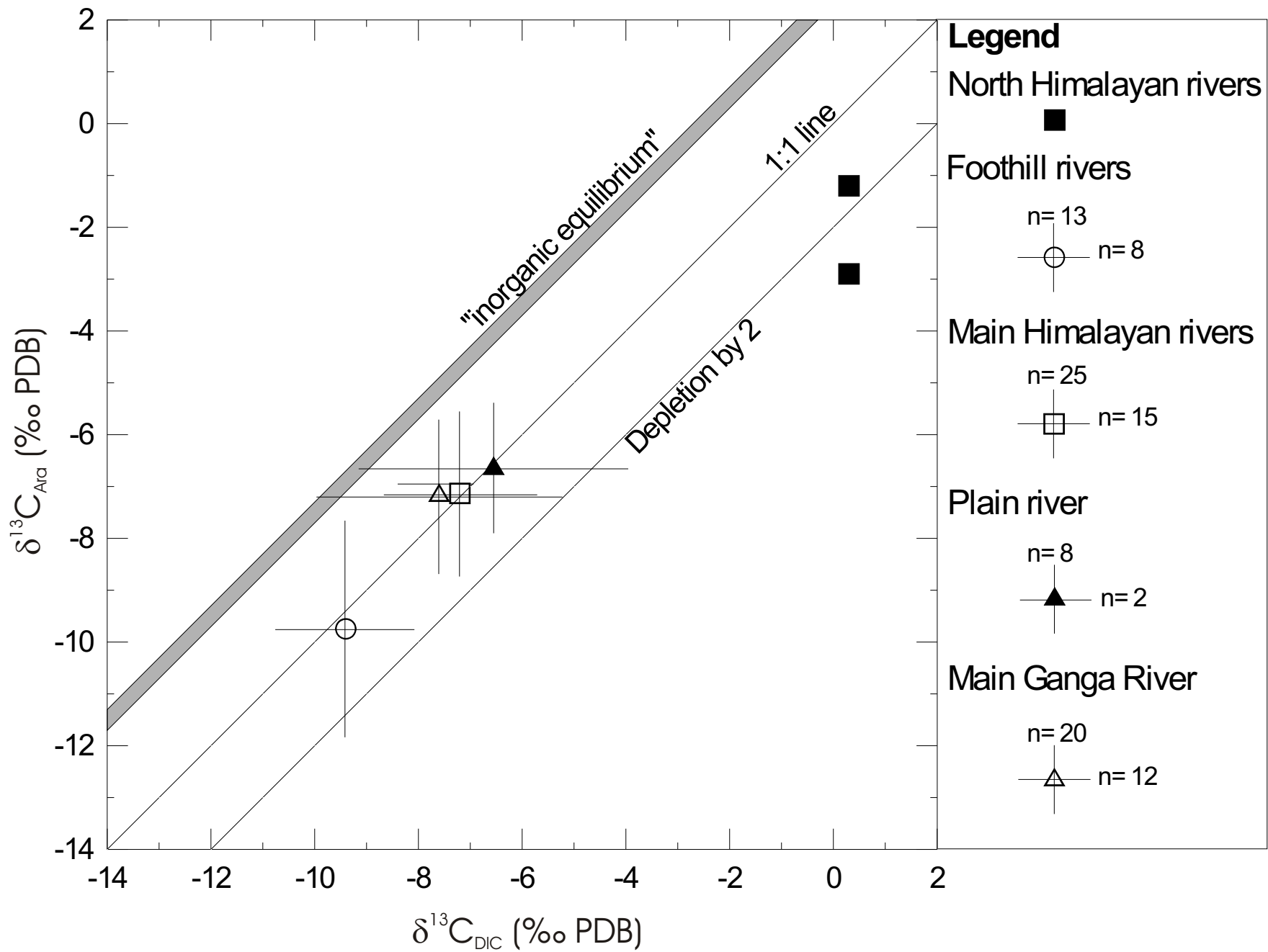


Fig 13 Edited Gajurel et al. (WPL)

Table 1a

Assays on Whole shell	$\delta^{13}\text{C}$ (PDB) ‰	$\delta^{18}\text{O}$ (VSMOW) ‰
No treatment	-5.8	28.7
No treatment	-5.8	28.7
370°C/1hr	-5.9	28.4
370°C/1hr	-5.8	28.6
370°C/1hr	-5.8	28.4
Plasma	-5.9	28.5
Plasma	-5.8	28.5
Plasma	-5.8	28.5
Mean	-5.8	28.6
Standard error	0.016	0.042
Standard deviation	0.02	0.12

Table 1b

Assays on Whole sample	$\delta^{13}\text{C}$ (PDB) ‰	$\delta^{18}\text{O}$ (VSMOW) ‰
No treatment	7.3	22.8
No treatment	7.3	22.9
No treatment	7.3	22.8
370°C/1hr	7.3	22.8
370°C/1hr	7.3	22.8
370°C/1hr	7.2	22.6
Plasma	7.3	22.8
Plasma	7.3	25.1
Mean	7.3	23.1
Standard error	0.013	0.291
Standard deviation	0.04	0.82

Table 2

Sample#	River / tributary	Location	Date	Elevation (m)	pH	Temperature (°C)	$\delta^{18}\text{O}$ (SMOW) ‰	δD (SMOW) ‰	$\delta^{13}\text{C}_{\text{DIC}}$ (PDB) ‰	$[\text{CO}_2]$ $\mu\text{ mol/l}$
North Himalaya										
LO 63	Tsarang Khola	Tsarang	May.20.90	3920		4.5	-18.8	-141.1	-0.3*	2770
LO 25	Nangyal Khola	Lo Manthang	May.19.90	3695			-17.3	-128.4	-6.7*	2080
Jomw 1	Kagbeni Khola	Muktinath	Mar.14.04	3576	7.5	7	-15.9	-108.2	na	
NH 133	Kali Gandaki	Lo Mantang	Apr.29.91	3575	7.8*	8.4	-15.9	-113.4	-3.2*	2513
LO 49	Kali Gandaki	Lo Manthang	May.19.89	3550		5	-16.2	-121.7	1.3*	2900
LO 15	Ghami Khola	Ghami	May.18.89	3450		6.3	-18.3	-133.6	-4.3*	2800
LO 23	Tsarang Khola	Tsarang	May.18.89	3430			-17.2	-130.6	1.4*	3960
LO 96	Narsing khola	Chhuksang	May.23.89	2900		10	-14.3	-107.0	3.9*	2450
NAG 21	Kali Gandaki	Kagbeni	Nov.25.95	2790	8.5*	3.8	-17.5	-132.5	0.4*	2567
Jomw 3	Terrace Kali	Jomsom	Mar.15.04	2750	8.1	9.6	-14.8	-104.0	na	
Jomw 4	Terrace Kali	Jomsom	Mar.15.04	2750		9.5	-12.9	-94.7	na	
99kg22	unnamed	Jomsom		2750			-15.7	-115	na	
Jomgw-7	unnamed	Jomsom	May.25.04	2731		15	-11.7	-85.5	na	
Jomw 5	Syan Khola	Jomsom	Mar.16.04	2730		15	-12.4	-83.3	na	
NH 147	Kali gandaki	Jomsom	May.5.91	2675	8.4*	8.4	-15.5	-113.4	0.3*	2513
LO 99	Thini khola	Kali	May.25.89	2650			-13.7	-92.1	-2.1*	2490
LO 103	Marpha khola	Marpha	May.25.89	2650			-8.6	-50.7	-5.0*	110
LO 101	Kali Gandaki	Marpha	May.25.89	2630		10	-14.2	-102.3	-1.4*	2340
NAG 30	Kali Gandaki	Chairogaon	Dec.1.95	2626	9.3*	6.3	-16.8	-124.7	0.3*	3093
99kg23	unnamed			2600			-11.2	-76	na	
NAG 32	Kali Gandaki	Tukuche	Dec.2.95	2530	8.8*	2.0	-16.4	-120.5	0.1*	2687
99kg24	Yamkin Khola			2500			-13.4	-92		
MO 500	Kali Gandaki	Khobang	Jul.25.94	2490	8		-17.7	-129.1	-1.1	1370
Jomw 6	Larjung Khola	Larjung	Mar.17.04	2460		14.5	-10.0	-63.8	na	
99kg26	Larjung Khola	Larjung		2440			-12.2	-84		
Foothills										
Gokarna	Bagmati	Kathmandu	May.95	1360		15	-7.0	-44.8	-11.7	565
17 ^J	Bagmati	Gokarna	Aug-Sept 86	1315			-10	-70.6	na	
19 ^J	Bishnumati	Balaju	Aug-Sept 86	1301			-9.1	-67	na	
22 ^J	Manohara	Lohakanthali	Aug-Sept 86	1297			-8.6	-65.6	na	

18 ^J	Bagmati	Minbhawan	Aug-Sept 86	1292			-10	-68	na	
23 ^J	Hanumante	Thimi	Aug-Sept 86	1291			-7.4	-59.4	na	
LO 402	Bishnumati	Teku		1285			-9.4		na	2613
20 ^J	Bishnumati	Teku	Aug-Sept 86	1285			-8.8	-68.5	na	
LO 400	Bagmati	Patan		1280			-8.8		na	
LO 401	Bagmati	Thapathali		1278			-8.7		na	
21 ^J	Nakhu	Nakhu	Aug-Sept 86	1275			-10.1	-73	na	
16 ^J	Bagmati	Chobhar	Aug-Sept 86	1270			-10.1	-73.5	na	
NAG 3	Bijayapur	Kundahar	Nov.11.95	870	8.1	20.6	-10	-68.6	-10.3	1750
MO 311	Andhi		Jul.8.98	850	8.2	29	-9.2	-63.4	na	980
MO 524	Phewa Lake	Pokhara	Jul.28.94	798			-8.2	-53.4	-8.5	380
APL 1	Phewa Lake	Pokhara	Jan.18.04	798		17.5	-8.5	-55.9	na	
PHL 1	Phewa Lake	Pokhara	Jan.18.04	798	7.5	17	-6.4	-43.0	na	
99kg49	unnamed			820			-9.2	-67	na	
NH 3	Surai khola	Tatopani	Mar.10.91	631	8.5*	18	-7.8	-39.0	-8.6*	6514
Btw-2	Tinau Khola	Charchare	Jan.6.01	559			-8.1		na	
99kg51	unnamed	Kerabari		480			-8.1	-60	na	
MO 327	Ransing Khola		Jul.8.94	385	8.4		-10.9	-78.0	-10.6	2990
94-03	Ransing Khola	Charang	Mar.5.94	385			-5.5	-36.7	na	
BakaiKR-3	Bakiya Khola	Chatiwani	Feb.17.01	265	7.2		-6.4		na	
94-18	Bankas Khola		Mar.29.94	250			-5.9	-39.3	na	
MO 321	Kweli Khola		Jul.9.98	250	8.2		-9.1	-64.9	-8.8	2775
94-02	Surai Khola		Mar.4.94	240			-6.1	-40.4	na	
MO 325	Surai Khola		Jul.8.94	240	8.4		-10.1	-71.1	-8	3630
94-01	Chor Khola		Mar.2.94	220			-6.8	-44.2	na	
94-17	Kachali Khola		Mar.29.94	220			-5.8	-43.5	na	
94-13	Gadel Khola	Palait	Mar.23.94	220			-6	-43.3	na	
94-14	Basunti Khola	Bashanti	Mar.24.94	220			-6.5	-42.5	na	
MO 317	Tinau Khola	Butwal	Jul.7.94	180	8.4		-11.4	-80.5	-8.5*	1500
Main Himalayan rivers										
LO 308	Narayani	Nayaran Ghat	Jun.9.93	190		26	-8.1	-50.6	-8.0*	1679
NAG 49	Narayani	Nayaran Ghat	Dec.11.95	190	8.4*	18.8		-69.5	-7.1*	2207
MO 330	Narayani	Nayaran Ghat	Jul.9.94	190	8.4		-10.9	-75.3	-7.6*	1430
NH 1	Narayani	Nayaran Ghat	Mar.9.91	190	8.5*	20	-10.7	-69.5	-5.6*	2320
PB 53	Narayani	Nayaran Ghat	Jul. 11.05	190					-7.9	1600

PB 81	Karnali	Chisopani	Jul. 15.05	190							-7.0	1480
8 ^R	Ghaghara	Ayodhya	Mar.82	98			-8.4	-54	na			
8 ^R	Ghaghara	Ayodhya	Sept.82	98			-9.4	-70	na			
BR 354	Ghaghara	Ayodhya	May.14.00	98	8.2	29.5	-7.6	-51.8	-6.1			3170
Kosi-1	Kosi	Kosi Barrage	May.1.04	84			-9.6	-63.4	na			
Kosi-2	Kosi	Kosi Barrage	May.21.04	84			-9.7	-63.5	na			
BR 363	Rapti	Gorakhpur	May.14.00	81	8.3	31.8	-3.0	-22.8	-6.30			4040
BR 334	Gandak	Barauli	May.10.00	67	8.1	31.7	-8.2	-53.3	-6.2			2680
BR 342	Ghaghara	Revelganj	May.11.00	56	8.2	30.4	-6.4	-46.1	-4.8			3480
18 ^R	Gandak	Hajipur	Mar.82	45			-8.9	-63	na			
18 ^R	Gandak	Hajipur	Sept.82	45			-10.2	-66	na			
BR 311	Gandak	Hajipur	May.5.00	45	8.0		-7.9	-51.3	-7			2280
BR 115	Gandak	Hajipur	Aug.7.01	45			-9.8	-66.8	-8.2			
PB 71	Kosi	Hydropower st.	Jul. 13.05	180					-10.2			780
BR 327	Kosi	Dumari Ghat	May.9.00	38	7.9	31.4	-7.2	-47.1	-7.3			1910
BR 101	Sapt Kosi		Aug.5.01	38			-10.7	-74.9	-9.2			
Plain river												
BR 134	Gomti		Aug.9.01	74			-7.4		na			
BR 375	Gomti		May.15.00	68	8.6	34.0	-6.3	-46.3	-4.7			4290
BR 135	Gomti		Aug.9.01		8.2		-6.4	-48.7	-8.4			
14 ^R	Gomti	Dobni	Mar.82				-7.1	-48	na			
Main Ganga River												
BR 350	Ganga	Allahabad	May.13.00	103	8.5		-3.6	-30.9	-2.6			3810
11 ^R	Ganga	Allahabad	Mar.82	103				-39	na			
11 ^R	Ganga	Allahabad	Sept.82	103				-69	na			
BR 388	Ganga	Varanasi Ghat	May.16.00	75	8.3	32.1	-7.6	-31.4	-4.1			4800
BR 141	Ganga	Varanasi	Aug.10.01	75	8.3		-6.2	-50.7	-8.9			
13 ^R	Ganga	Varanasi	Dec.82	75				-39	na			
13 ^R	Ganga	Varanasi	Mar.82	75				-55	na			
BR 126	Ganga	Patna	Aug.8.01	45			-6.8	-46	-9.1			
17 ^R	Ganga	Patna	Dec.82	45				-41	na			
16 ^R	Ganga	Patna	Mar.82	45				-35	na			
17 ^R	Ganga	Patna	Mar.82	45			-3.8	-39	na			
17 ^R	Ganga	Patna	Sept.82	45			-10.6	-73	na			
BR 309	Ganga	Patna Ghat	May.6.00	45	8.1	29.0	-7	-34.1	-6.9			3720

BR 112	Ganga	Manihari	Aug.6.01	38			-9	-62	-9	
BR 318	Ganga	Rajmahal	May.8.00	28	8.1	30.9		-41.8	-6	3150
BGP 65	Ganga	Rajshahi	Mar.2.93	20	8.5*	23.6	-7.7		-8.2*	4321
BGP 4	Ganga	Rajshahi	Aug.1.92	20	7.6*	30.7	-8.7	-62.6	-10.1*	1711
BR 410	Ganga	Harding Bridge	Jul.31.04	17			-6.8	-42.1	-7.3	1500
BR 213	Ganga	Harding Bridge	Jul.7.02	17			-10	-69.7	-9.2	
BR 521	Ganga	Harding Bridge	Jul. 23.05	17					-9.8	1870
Water from ponds										
Bug-1	Rice field	Kathmandu	Jul.20.02	1441		30	-6.8		na	
MKR-1a	Small pond	Kathmandu	Feb.5.01	1230	6.9	8	3.4		na	
Btw-3	Small pond	Bastadi	Jan.10.01	855	7.6	12	-5.1		na	
RangsingKR	Ditch	Ransin	Feb.19.01	325		22	-1.9		na	
MaghaK	Small pond	Kairmara	Dec.13.01	190			-3.8		na	
BakaiKR-1	Small pond	Khoria	Feb.16.01	190	7.2	22	-4.9		na	
BR 370	Rapti pond	Unwal	May.14.00	81			5.6	14.1	-4.2	5110
BR 341	Gandak pond	Barauli	May.10.00	67			2.4	-2.5	-3.6	4760

* Data from Galy and France-Lanord, (1999), 99kg22 corresponds to data Garziona et al., (2000b); 17^J corresponds to data Jenkins et al., (1987) and 17^R corresponds to data Ramesh and Sarin, (1992).

Table 3

Sample #	River /Location	Elevation (m)	Shell $\delta^{13}\text{C}$ (PDB) ‰	Shell $\delta^{18}\text{O}$ (PDB) ‰	Genus/ Species
North Himalaya					
Jomg 3	Kali G./ Jomsom	2750	-1.2	-14.5	<i>Lymnaea</i> sp
Jomg 4	Kali G./ Jomsom	2750	-2.9	-11.9	<i>Lymnaea</i> sp.
Jomg 7	Kali G./ Jomsom	2731	-7.1	-10.8	<i>Lymnaeinae</i> sp.
Jomg 5	Kali G./ Jomsom	2730	-8.3	-9.4	<i>Lymnaeinae</i> sp.
Jomg 6	Kali G./ Jomsom	2560	-6.9	-7.3	<i>Lymnaea</i> sp
Phewa Lake					
Phewa-1	Pokhara	798	-11.2	-9.1	<i>Melanoides cf. tuberculata</i>
Phewa-2	Pokhara	798	-10.9	-9.8	<i>Bellamyia bengalensis</i>
Phewa-3	Pokhara	798	-6.5	-8.3	<i>Lamellidens</i> sp.
Phl1a	Pokhara	798	-6.8	-7.3	<i>Bellamyia bengalensis</i>
Phl1b	Pokhara	798	-6.5	-9.1	<i>Indoplanorbis</i> sp.
Apg 1a	Pokhara	798	-5.7	-7.9	<i>Bellamyia bengalensis</i>
Apg 1b	Pokhara	798	-6.6	-8.4	<i>Melanoides cf. tuberculata</i>
<i>Average</i>			-7.7	-8.6	
<i>Standard deviation</i>			2.3	0.8	
Foothill rivers					
Btw-2	Tinau/ Charchare	559	-9.6	-8.8	<i>Bithynia</i> sp.
Btw-2 Melano	Tinau/ Charchare	559	-11.4	-9.7	<i>Melanoides cf. tuberculata</i>
Btw-2 cor	Tinau/ Charchare	559	-11.2	-8.7	<i>Corbicula</i> sp.
0027 a	Babai/ Tulsipur	555	-7.3	-7.4	<i>Bellamyia bengalensis</i>
0027 b	Babai/ Tulsipur	555	-7.4	-7.1	<i>Corbicula</i> sp.
0027 c	Babai/ Tulsipur	555	-8.7	-7.6	<i>Indoplanorbis</i> sp.
0027 d	Babai/ Tulsipur	555	-8.7	-6.2	<i>Gyraulus</i> sp.
0027 e	Babai/ Tulsipur	555	-7.7	-7.6	<i>Melanoides cf. tuberculata</i>
BakaiKR-2	Simat/ Chatiwan	270	-11.2	-7.7	<i>Melanoides cf. tuberculata</i>
BakaiKR-3	Bakiya/ Chatiwan	265	-13.2	-5.9	<i>Lymea acumita</i>
Ga 126	Diyalobanglo Khola/ Diyalobanglo	165	-13.4	-6.5	<i>Melanoides cf. tuberculata</i>
Chit-1	Rapti/ Megghauli	145	-8.2	-7.3	<i>Brotia</i> sp.
Chit-3	Rapti/ Megghauli	145	-8.7	-8.9	<i>Indoplanorbis</i> sp.
<i>Average</i>			-9.7	-7.6	
<i>Standard deviation</i>			2.1	1.1	
Main Himalayan rivers					
Ga 1j	Narayani/ Narayangad	178	-8.2	-6.2	<i>Brotia</i> sp.
Ga 1	Narayani/ Narayangad	178	-6.9	-8.3	<i>Brotia</i> sp.
Ga g	Narayani/ Narayangad	140	-9.5	-6.6	<i>Gastopoda</i> sp.
Koshi-1	Kosi Dam/ Nepal	84	-4.7	-6.8	<i>Indoplanorbis exustus</i>
Koshi-2	Kosi Dam/ Nepal	84	-9.1	-11.5	<i>Melanoides cf. tuberculata</i>
Koshi-3	Kosi Dam/ Nepal	84	-10.9	-11.4	<i>Bellamyia bengalensis</i>
BR 373a	Ghaghara/ Dohrighat	74	-7.3	-4.3	<i>Bellamyia bengalensis</i>
BR 373b	Ghaghara/Dohrighat	74	-7.4	-11.4	<i>Bellamyia bengalensis</i>
BR 373-0	Ghaghara/ Dohrighat	74	-4.4	-7.9	<i>Digoniostoma textum</i>
BR 373-0'	Ghaghara/ Dohrighat	74	-6.1	-9.7	<i>Digoniostoma textum</i>
BR 373-1	Ghaghara/ Dohrighat	74	-5.4	-6.6	<i>Digoniostoma textum</i>

BR 373-2	Ghaghara/ Dohrighat	74	-8.6	-11.4	<i>Digoniostoma textum</i>
BR 373-3	Ghaghara/ Dohrighat	74	-7.2	-9.2	<i>Digoniostoma textum</i>
BR 373-4	Ghaghara/ Dohrighat	74	-6.2	-11.4	<i>Digoniostoma textum</i>
BR 373-5	Ghaghara/ Dohrighat	74	-7.4	-10.7	<i>Digoniostoma textum</i>
BR 373-6	Ghaghara/ Dohrighat	74	-5.2	-8.9	<i>Indoplanorbis</i> sp.
BR 373-7	Ghaghara/ Dohrighat	74	-7.0	-11.0	<i>Indoplanorbis</i> sp.
BR 373-8	Ghaghara/ Dohrighat	74	-5.0	-9.6	<i>Indoplanorbis</i> sp.
BR 373-9	Ghaghara/ Dohrighat	74	-5.9	-10.6	<i>Indoplanorbis</i> sp.
BR 373-10	Ghaghara/ Dohrighat	74	-5.5	-7.5	<i>Indoplanorbis</i> sp.
BR 337a	Gandak/ Barauli	67	-7.3	-4.2	<i>Bellamyia bengalensis</i>
BR 337a apex	Gandak/ Barauli	67	-9.7	-4.8	<i>Bellamyia bengalensis</i>
BR 337b	Gandak/ Barauli	67	-7.7	-10.0	<i>Bellamyia bengalensis</i>
BR 337c	Gandak/ Barauli	67	-7.3	-9.9	<i>Bellamyia bengalensis</i>
BR 333a	Kosi/ Dumarighat	35	-8.4	-9.1	<i>Bellamyia</i> sp.
<i>Average</i>			-7.1	-8.8	
<i>Standard deviation</i>			1.7	2.3	
Plain river					
BR 367a	Rapti/ Gorakpur	81	-7.2	-6.8	<i>Bellamyia</i> sp.
BR 134b	Gomti	74	-7.8	-8.0	<i>Corbicula</i> sp.
BR 134c	Gomti	74	-5.4	-5.1	<i>Bellamyia</i> sp.
BR 134d	Gomti	74	-6.3	-8.0	<i>Corbicula</i> sp.
BR 134e	Gomti	74	-7.6	-7.1	<i>Bellamyia bengalensis</i>
BR 134f	Gomti	74	-4.1	-6.1	<i>Melanoides cf. tuberculata</i>
BR 134g	Gomti	74	-7.1	-7.1	<i>Bellamyia</i> sp.
BR 376a	Gomti	68	-7.2	-7.6	<i>Bellamyia</i> sp.
<i>Average</i>			-6.6	-7	
<i>Standard deviation</i>			1.3	1.0	
Main Ganga River					
BR 385a	Ganga/ Varanasi	75	-6.0	-5.9	<i>Bellamyia bengalensis</i> .
BR 143g	Ganga/ Varanasi	75	-6.8	-5.1	<i>Bellamyia bengalensis</i>
BR 143b	Ganga/ Varanasi	75	-5.1	-5.6	<i>Corbicula</i> sp.
BR 143c	Ganga/ Varanasi	75	-5.3	-5.0	<i>Bellamyia bengalensis</i>
BR 143d	Ganga/ Varanasi	75	-6.4	-5.3	<i>Corbicula</i> sp.
BR 305a	Ganga/ Patna	45	-10.1	-8.6	<i>Brotia</i> sp.
BR 316a	Ganga/ Barauni	38	-5.5	-7.0	<i>Bellamyia bengalensis</i>
BR 316b	Ganga/ Barauni	38	-6.6	-7.1	<i>Bellamyia bengalensis</i>
BR 316-1	Ganga/ Barauni	38	-7.9	-7.2	<i>Bellamyia bengalensis</i>
BR 316-2	Ganga/ Barauni	38	-7.3	-7.2	<i>Bellamyia bengalensis</i>
BR 316-3	Ganga/ Barauni	38	-6.9	-6.0	<i>Bellamyia bengalensis</i>
BR 316-4	Ganga/ Barauni	38	-7.2	-7.0	<i>Bellamyia bengalensis</i>
BR 316-5	Ganga/ Barauni	38	-7.3	-7.1	<i>Bellamyia bengalensis</i>
BR 316-6	Ganga/ Barauni	38	-7.0	-6.1	<i>Bellamyia bengalensis</i>
BR 316-7	Ganga/ Barauni	38	-5.9	-7.0	<i>Bellamyia bengalensis</i>
BR 316-8	Ganga/ Barauni	38	-5.9	-7.1	<i>Bellamyia bengalensis</i>
BR 316-9	Ganga/ Barauni	38	-7.2	-6.4	<i>Bellamyia crassa</i>
BR 316-10	Ganga/ Barauni	38	-8.1	-7.8	<i>Bellamyia bengalensis</i>
BGP 4e Bro	Ganga/ Harding	20	-10.3	-5.2	<i>Brotia</i> sp.
BGP 4e	Ganga/ Harding.	20	-9.6	-4.5	<i>Bellamyia bengalensis</i>
<i>Average</i>			-7.1	-6.4	

	<i>Standard deviation</i>		1.5	1.0	
Himalayan ponds					
Bug-1	Kathmandu Valley	1441	-11.6	-6.7	<i>Lymnaea</i> sp.
Bug-2	Kathmandu Valley	1441	-12.5	-7.4	<i>Bithynia</i> sp.
Bug 2op	Kathmandu Valley	1441	-11.5	-6.8	<i>Opercula</i> of <i>Bithynia</i> sp.
MKR-1a	Kathmandu Valley	1230	-0.8	2.4	<i>Lymnaea</i> sp.
MKR-1b	Kathmandu Valley	1230	2.5	-6.8	<i>Indoplanorbis</i> sp.
MKR-1c	Kathmandu Valley	1230	0.6	-3.4	<i>Physa</i> sp.
Tau-1	Kathmandu Valley	1290	-8.0	-7.6	<i>Lymnaea</i> sp.
0027 f	Dun Valley/ Nepal	555	-8.3	-3.6	<i>Gastopoda</i> sp.
0027 g	Dun Valley/ Nepal	555	-7.1	3.6	<i>Bithynia</i> sp.
0027 h	Dun Valley/ Nepal	555	-9.3	2.8	<i>Lymnaea</i> sp.
Chit-2	Dun Valley/ Nepal	145	-7.6	-3.8	<i>Bellamya bengalensis</i>
Ganga plain ponds					
BakaiKR-1	Terai/ Nepal	190	-5.8	-2.3	<i>Bellamya bengalensis</i>
MaghaK	Terai/ Nepal	190	-12.6	-7.3	<i>Bellamya bengalensis</i>
BR 369a	Rapti/ Unwal	81	-4.7	-7.7	<i>Bellamya</i> sp.
BR 369b	Rapti/ Unwal	81	-4.4	-2.2	<i>Bellamya</i> sp.
BR 339a	Gandak/ Barauli	67	-7.3	-6.3	<i>Bellamya bengalensis</i>
BR 339b	Gandak/ Barauli	67	-5.6	-2.5	<i>Brotia</i> sp.
BR 339c	Gandak/ Barauli	67	-6.7	-2.3	<i>Bellamya bengalensis</i>

Table 4

Shell sample #	Intra-shell sample #.	Distance from apex (mm)	$\delta^{13}\text{C}$ (PDB) ‰	$\delta^{18}\text{O}$ (PDB) ‰
Chit-1	strie-1	141	-7.8	-7.5
	strie-2	129	-8.2	-8.0
	strie-3	118	-8.3	-7.8
	strie-4	106	-8.1	-7.6
	strie-5	95	-8.2	-6.9
	strie-6	84	-8.2	-7.0
	strie-7	73	-8.2	-7.0
	strie-8	61	-8.2	-6.9
	strie-9	51	-8.3	-7.1
	strie-10	38	-8.2	-7.1
	strie-11	28	-8.1	-7.2
Btw-2 cor	a	9.5	-11.0	-7.0
	b	8.5	-11.2	-7.8
	c	7.5	-11.8	-9.3
	d	5.5	-11.4	-9.8
	f	4	-10.9	-9.0
	e	2	-10.8	-9.3
BR 316-10	BR 316a	157	-7.7	-6.6
	BR 316b	152	-7.8	-6.5
	BR 316c	147	-8.1	-6.5
	BR 316 10d	141	-8.1	-6.3
	BR 316 10d'	138	-8.5	-6.5
	BR 316 10e	135	-8.0	-6.7
	BR 316 10f	130	-8.0	-6.6
	BR 316 10g	127	-8.2	-6.5
	BR 316 10h	123	-8.1	-6.6
	BR 316 10i	120	-8.1	-6.5
	BR 316 10j	118	-8.3	-6.9
	BR 316 10k	116	-8.1	-7.4
	BR 316 10l	112	-8.1	-7.6
	BR 316 10m	107	-8.2	-7.6
	BR 316 10n	102	-8.3	-8.1
	BR 316 10o	97	-8.4	-7.8
	BR 316 10p	94	-8.5	-8.0
	BR 316 10q	87	-8.4	-8.2
	BR 316 10r	81	-8.6	-7.7
	BR 316 10s	76	-8.7	-8.1
	BR 316 10t	70	-8.4	-8.2
	BR 316 10u	66	-8.1	-8.1
	BR 316 10v	61	-7.3	-9.2
	BR 316 10w	50	-7.0	-9.6
	BR 316 10x	46	-7.7	-8.4
	BR 316 10y	41	-8.1	-8.5
	BR 316 10z	38	-7.9	-9.2
BR 316 10aa	31	-8.0	-9.3	
BR 316 10ab	25	-8.2	-9.3	
BR 316 10ac	15	-7.9	-9.4	
BR 316 10ad	8	-8.0	-9.5	
BR 337	BR 337 3c	154	-12.3	-9.3
	BR 337 3d	152	-12.3	-8.5
	BR 337 3e	148	-12.5	-9.3
	BR 337 3f	144	-12.4	-9.1
	BR 337 3g	140	-12.5	-8.4
	BR 337 3h	136	-12.4	-8.2
	BR 337 3i	132	-12.4	-9.2
	BR 337 3k	128	-12.3	-9.5
	BR 337 3l	124	-12.9	-10.3

BR 337-3	BR 337 3m	120	-12.6	-9.7
	BR 337 3n	116	-12.1	-8.6
	BR 337 3o	112	-12.4	-9.4
	BR 337 3p	108	-12.6	-9.5
	BR 337 3q	104	-12.6	-9.6
	BR 337 3r	100	-12.6	-9.2
	BR 337 3s	96	-12.2	-10.7
	BR 337 3t	92	-12.7	-10.1
	BR 337 3v	84	-11.3	-10.6
	BR 337 3w	80	-12.0	-9.9
	BR 337 3x	76	-12.0	-9.8
	BR 337 3y	72	-12.1	-10.5
	BR 337 3A	65	-11.7	-11.1
	BR 337 3B	62	-11.0	-10.7
	BR 337 3C	58	-11.0	-9.4
	BR 337 3D	54	-11.0	-9.0
	BR 337 3F	33	-11.2	-10.1
	BR 337 3ag	26	-10.2	-10.2
BR 337 3ah	14	-10.6	-8.8	
